

CARBON DIOXIDE SEQUESTRATION VIA pH REDUCTION OF RED MUD USING LIQUID CO₂

Chunmei Shi, Jianhang Xu, Eric Beckman and Robert Enick
Chemical and Petroleum Engineering
1249 Benedum Engineering Hall
University of Pittsburgh
Pittsburgh, PA 15261

KEYWORDS: red mud, steel plant dust, carbon dioxide, carbonate

ABSTRACT

The pH of red mud, waste from the Bayer process for alumina manufacture, can be lowered by contacting the aqueous red mud slurry with liquid carbon dioxide. The carbonic acid that forms in the water in the presence of liquid CO₂ (pH of 2.8 - 2.9) neutralizes the basic compounds of the red mud via the formation of metal carbonates. The pH of a 45% red mud slurry can be reduced from 12.5 to a stable value of 9.0-9.5 via the contact of liquid CO₂ at 298 K and 6.7-10 MPa. The required reaction time is 5-15 minutes if the slurry is well mixed with the liquid CO₂. The carbonates were not removed from the red mud because pH reduction was the only process requirement. The approximate amount of sequestration is about 2.3 gr CO₂ per 100 gr dewatered red mud.

INTRODUCTION

The Bayer process, developed by Karl Josef Bayer 110 years ago, remains the most widely used means of manufacturing calcined commercial alumina from bauxite (40-60% Al₂O₃). Typically, the alumina in the crushed bauxite feed is dissolved aqueous caustic soda at high temperature. Red mud, the insoluble impurities of bauxite, is then separated from the soluble alumina and caustic soda and washed. The soluble sodium aluminate is then partially hydrolyzed, yielding an aluminum trihydroxide precipitate. Calcination of the aluminum trihydroxide yields the anhydrous alumina product (Anderson and Haupin 1985). Aluminum is subsequently produced by the electrolysis of alumina.

The major by-product from the Bayer process is red mud, the insoluble residue of the alumina extraction from the bauxite (Hind et al.1999, Prasad et al.1996). Approximately 70 million tons of red mud is generated annually throughout the world. Red mud disposal methods include traditional closed cycle disposal (CCD) methods and modified closed cycle disposal (MCCD). A new class of dry stacking (DS) technology has also emerged which requires much less land. Problems associated with the disposal of red mud waste include its high pH (12-13), alkali seepage into underground water, safety in storage, and alkaline air borne dust impact on plant life. Efforts to ameliorate red mud typically and possibly, use it as a raw material usually incorporate a pH-reduction processing step (Wong and Ho 1994, Vachon et al. 1994, Koumanova, et al. 1997, Rodriguez et al.1999). Various aqueous acidic solutions have been considered for this application, including acidic industrial wastewater (Wong and Ho 1994). The use of carbonic acid has also been considered. Gas phase CO₂ or CO₂-containing flue gas has been bubbled through aqueous slurries to form carbonic acid in the aqueous phase (Sziirmai, et al. 1991). The carbonic acid results with basic components of the red mud, lowering its pH. However, the pH of water exposed to gaseous CO₂ is not likely to drop below 5.5 (approximately), and hence the rate of reaction/neutralization of the solids in the aqueous slurry is typically not fast enough to satisfy industrial needs. At the short contact times which industrial process rates demand, only a fraction of the alkaline material in red mud is neutralized using gaseous CO₂. Hence although the pH of the aqueous phase drops rapidly upon exposure to CO₂ gas, it soon rises again to unacceptable levels as additional alkaline material leaches from the mud.

The focus of this investigation was the use of high-pressure *liquid* carbon dioxide, rather than *vapor phase* carbon dioxide, for the pH reduction of red mud. The pH of water in contact with liquid CO₂ is 2.80-2.95 over the 298-343 K temperature range and 70-200 atm pressure range (Toews, et al. 1995). This is significantly lower than the pH of 5.0-5.6 that can be attained with gas-phase carbon dioxide. Therefore, we expected that a more rapid and effective neutralization of the red mud would be achieved using liquid carbon dioxide. The apparatus used for this remediation would need to operate at elevated pressures, however.

MATERIAL AND METHODS

Dewatered red mud was provided by Alcoa. Its approximate composition is provided in Table 1.

Table 1. The Composition of the Red Mud Sample

Compound	Formula	Content In Red Mud	MW
Hematite	Fe_2O_3	10-30wt%	160
Alumino-geothite	$(\text{Fe,Al})\text{OOH}$	10-30	75
Sodalite	$3\text{Na}_2\text{O} \cdot 3\text{Al}_2\text{O}_3 \cdot 6\text{SiO}_2 \cdot \text{Na}_2\text{SO}_4$	4-40	994
Tricalcium aluminate	$3\text{CaO} \cdot \text{Al}_2\text{O}_3 \cdot 6\text{H}_2\text{O}$	2-20	378
Anatase/Rutile	TiO_2	2-15	80
Calcite	CaCO_3	2-10	100
Quartz	SiO_2	0-30	60
Boehmite	$\text{Al}_2\text{O}_3 \cdot \text{H}_2\text{O}$	0-20	120
Gibbsite	$\text{Al}_2\text{O}_3 \cdot 3\text{H}_2\text{O}$	0- 5	156
Kaolinite	$\text{Al}_2\text{O}_3 \cdot 2\text{SiO}_2 \cdot 2\text{H}_2\text{O}$	0- 5	258
Muscovite	$\text{K}_2\text{O} \cdot 3\text{Al}_2\text{O}_3 \cdot 6\text{SiO}_2 \cdot 2\text{H}_2\text{O}$	0-15	796

Two slurries were prepared from this sample by mixing it with distilled water. The 45wt% red mud and 10% red mud slurries had pH values of 12.5 and 11.8, respectively. The slurry was contacted with liquid carbon dioxide at 297 K and 10 MPa in an attempt to neutralize both the free soda and bound soda in the red mud. In a typical experiment, 40 gr of the slurry and 40 ml of liquid carbon dioxide at 297 K at 10 MPa psia were introduced to a variable volume, windowed cell. This amount of carbon dioxide used was sufficient to keep the aqueous phase saturated with CO_2 , and a clear liquid carbon dioxide phase resided above the slurry in each experiment. The system was then gently mixed via rocking throughout the duration of the treatment, which ranged from 1 minute to 4 hours, at 297 K and 10 MPa. After specified reaction time had elapsed, the mixing was stopped and the liquid CO_2 was slowly vented from the top of the vessel.

In order to estimate the amount of liquid CO_2 that was sequestered during this experiment, a non-sampling, CO_2 material balance experiment was conducted. The initial pressure of this experiment was set at 5000 psia. In the control experiment, only water and CO_2 were introduced to the cell. The pressure in the cell dropped due to cooling of the vessel (which was heated as the CO_2 was compressed into the sample volume) and dissolution of the CO_2 into the aqueous phase. The experiment was then repeated with the same amount of water and carbon dioxide, but with a specified amount of dewatered red mud. The pressure in the vessel dropped more rapidly and reached a lower limiting value due to the neutralization reaction that removed CO_2 from the liquid phase and transformed it into a carbonate via the formation of carbonic acid and reaction in the aqueous phase. The additional pressure drop, temperature, initial pressure, knowledge of CO_2 density as a function of temperature and pressure and volume of liquid CO_2 , were then used to perform a material balance that indicated the amount of CO_2 that formed carbonates.

A one-liter fixed volume cell with turbine impeller mixing was employed for the neutralization experiments because of the poor mixing observed during the rocking of the smaller, variable volume view cell. Approximately 900 gr of the 45% red mud slurry was introduced to this vessel, which was then blanketed with liquid carbon dioxide. The aqueous slurry and the liquid carbon dioxide were mixed at 297 K and 6.7 MPa using several axial flow impellers spinning at 300 rpm.

RESULTS

The pH reduction results for the smaller vessel with mixing by rocking are illustrated in Figures 1 and 2. The results, shown on the following figures, indicate that

- (1) there is a reduction in pH immediately following the exposure to liquid CO_2 ,
- (2) the pH slowly rises and then levels off following the treatment due to the release of bound soda via desilication,
- (3) the 10% red mud slurries approached an equilibrium pH of approximately 9, regardless of the duration of the mixing
- (4) the efficiency of the treatment was comparable for all of the 10wt% red mud slurries
- (5) the 45% red mud slurries approached an equilibrium value, with lower pH values attained for solutions that were mixed for longer times during treatment (e.g. 4 hr. of mixing was required to attain an equilibrium pH of 9

The material balance experimental results are shown in Figure 3. The difference between the curves represents a "sequestration" of carbon dioxide. Using the data at 5000 minutes, approximately 2.3 grams of CO₂ can be sequestered for each 100 grams of dewatered red mud.

The effect of neutralizing the red mud with more vigorous mixing is shown in Figure 4. Reaction times of 5-15 minutes were capable of lowering the ultimate pH value to approximately 9.5, as opposed to the 4 hours required to lower the pH to 9 with poor mixing (Figure 2). The pH of the treated mud reached its equilibrium value within two weeks of treatment as shown in Figure 4, while several months were required for equilibration of the sample that was poorly mixed (Figure 2).

DISCUSSION

The neutralization of red mud can be achieved with liquid carbon dioxide at ambient temperature due to the pH value of carbonic acid at high pressure being in the 2.8 - 2.9. As expected and previously reported for red mud treated with gaseous CO₂, the pH of the red mud was close to 7 immediately after the treatment, it soon rose again as additional alkaline material leached from the mud. Effective treatment was obtained within minutes by reducing mass transfer limitations with vigorous mixing with impellers, rather than rocking the contents of the vessel. The process simultaneously remediated the red mud while sequestering about 2% (based on dewatered red mud mass) CO₂. The process requires the use of high pressure, corrosion resistant equipment, however, and power for the operation of the high-pressure pumps.

CONCLUSIONS

Liquid carbon dioxide was more effective for pH reduction of red mud than vapor phase CO₂ because carbonic acid pH values less than 3 can be realized with high-pressure carbon dioxide (6.7 - 10 MPa in this study). The initial red mud pH of 12-13 was lowered to 7-8 immediately after treatment, then slowly rose to values of 9.0-9.5 due to desilication reactions of the treated red mud. The processing time was reduced to 5-15 minutes using vigorous mixing of the liquid carbon dioxide and aqueous red mud slurry. Approximately 2 gr of carbon dioxide per 100 gr of red mud were bound in carbonate products when the process was conducted at 297 K.

ACKNOWLEDGMENTS

We would like to thank Normex International for their financial support of this work. We would also like to thank Alcoa for supplying red mud samples.

REFERENCES

- Anderson, W.A., Haupin, W.E., "Aluminum and Aluminum Alloys," in the Kirk-Othmer Concise Encyclopedia of Chemical Technology, Wiley and Sons, New York (1985)
- Hind A.R., Bhargava, S.K., Grocott, S.C., *Colloids Surface*, 146: (1-3) 359-374 Jan 5, 1999
- Koumanova, B., Drame, M., Popangelova, M., *Resources Conservation and Recycling*, 19: (1) 11-20 Jan 1997
- Prasad, P.M., Chandwani, H.K., Mahadevan, H., *Transactions of Indian Institute of Metals*, 49: (6) 817-839 Dec 1996.
- Rodriguez, G., Rivera, F., Pendas, S., *Boletin De La Espanola De Ceramica Y Vidrio* 38: (3) 220-226 May-Jun 1999
- Szirmai, E., Babusek, S., Balogh, G., Nedves, A., Horvath, G., Lebenyi, Z., Pinter, J., "Method for the Multistage, Waste-free Processing of Red Mud to Recover Basic Materials of Chemical Industry," US Patent 5,053,144, Oct. 1 1991
- Vachon P, Tyagi R., Auclair J., Wilkinson K., *Environmental Science & Technology*, 28: (1) 26-30 Jan 1994
- Wong, J., Ho, G., *Soil Science*, 158: (2) 115-123 Aug 1994

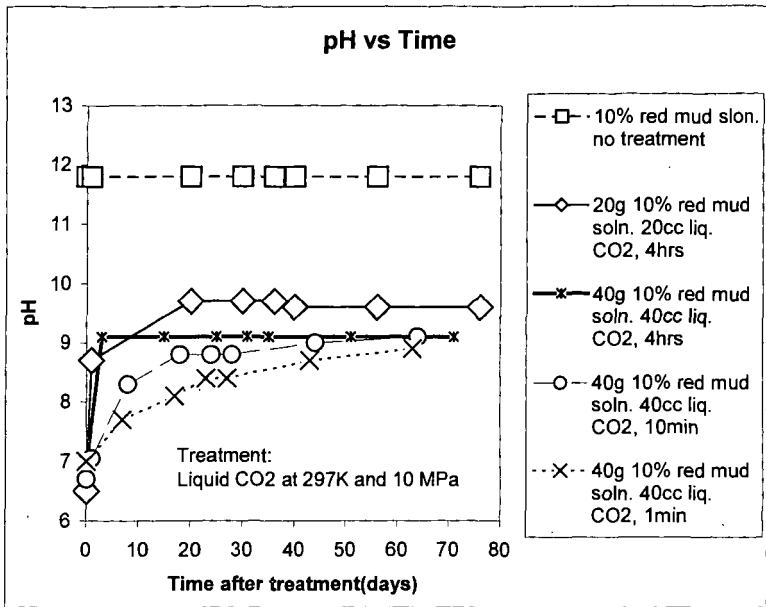


Figure 1. pH reduction of 10% Red Mud Slurries, Small Vessel, Poor Mixing via Rocking

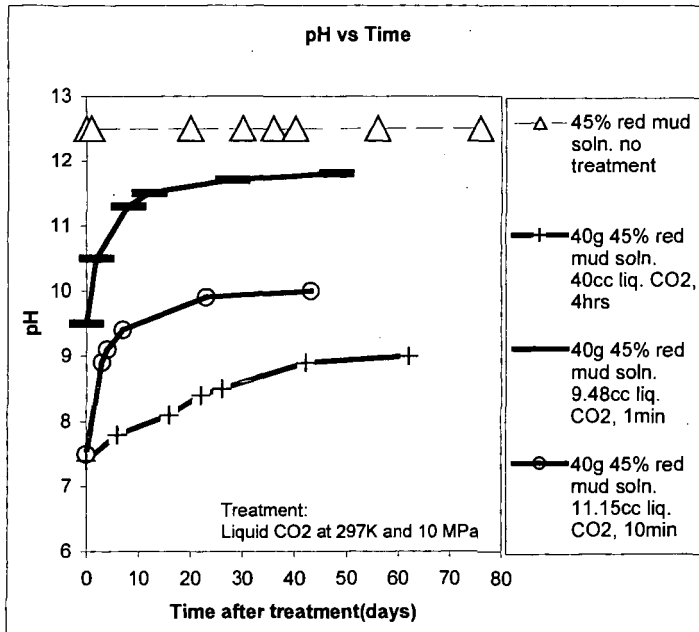


Figure 2. pH Reduction of 45% Red Mud Slurries, Small Vessel, Poor Mixing via Rocking

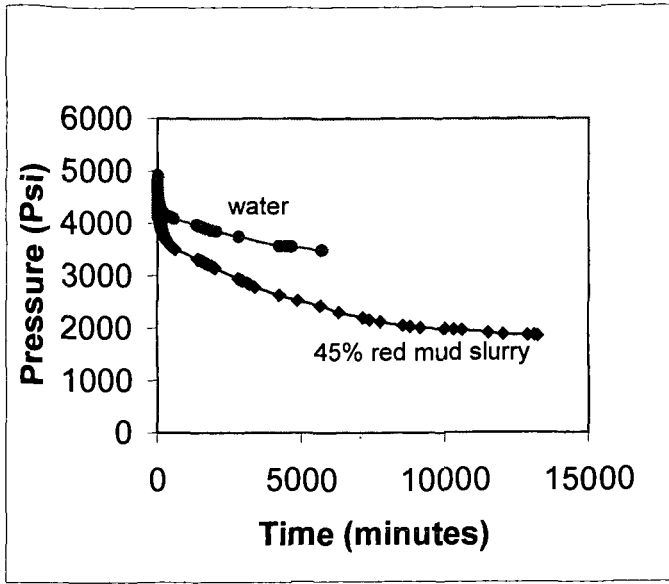


Figure 3. Pressure Decline Measurements at 298 K, 10 ml CO₂, 43 gr Water, Difference Between the Curves Corresponds to the CO₂ in Liquid CO₂ that Formed Carbonates

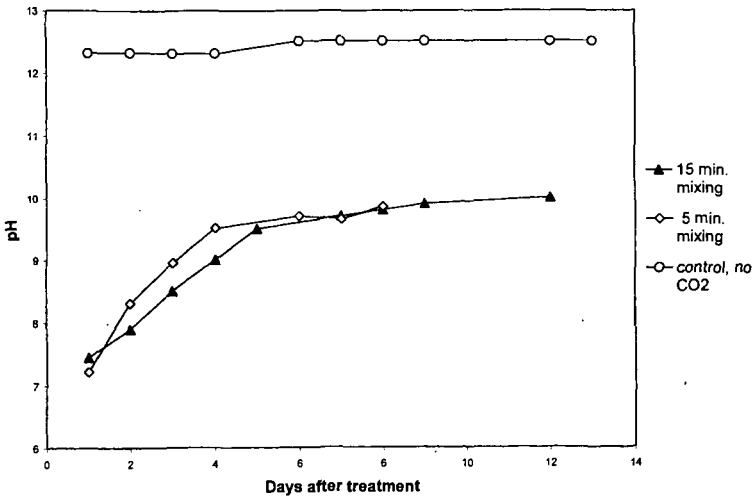


Figure 4. pH Reduction of 45% Red Mud Slurries, Large Vessel, Vigorous Mixing with Impellers, 900g slurry, 130g CO₂, 6.7 MPa

CARBON DIOXIDE STORAGE AS MINERAL CARBONATES

Daniel J. Fauth, Philip M. Goldberg, James P. Knoer, and Yee Soong
U. S. Department of Energy, National Energy Technology Laboratory (NETL)
Pittsburgh, PA 15236-0940

William K. O'Connor, David C. Dahlin, David N. Nilsen, and Richard P. Walters
U.S. Department of Energy, Albany Research Center (ARC)
Albany, Oregon 97321

Klaus S. Lackner and Hans-Joachim Ziock
Los Alamos National Laboratory (LANL)
Los Alamos, New Mexico 87545

Michael J. McKelvy
Arizona State University (ASU)
Tempe, Arizona 85287-1704

Zong-Ying Chen
Science Applications International Corporation (SAIC)
Pittsburgh, PA 15236

KEYWORDS: CO₂ sequestration, magnesium silicate, mineral carbonation

INTRODUCTION

The sequestration of greenhouse gas emissions in the 21st century, in particular carbon dioxide (CO₂), will have a profound influence on the environmental impact of electric power systems within the United States and abroad. Within the U. S., nearly one-third of all anthropogenic or human-caused CO₂ emissions are generated by electric power systems estimated at 6 GtC/year (1). Large economic benefits will continue for the U.S., when and how CO₂ sequestration technologies will be implemented, thus, securing inexpensive and plentiful sources of fossil-fuel-based electric power.

As participants in the Mineral Carbonation Study Program within the United States Department of Energy (DOE), the Mineral Carbonation Research Cluster has focused its carbon sequestration efforts on developing a long-term mitigation strategy. Our approach employs reacting abundant magnesium-rich silicate minerals in an exothermic reaction with CO₂ forming thermodynamically stable and environmentally benign mineral carbonate products. Drawing on mineral carbonation to reduce CO₂ emissions has a myriad of potential advantages. Mineral carbonation mimics the natural weathering of rock. Mineral carbonates, the principal product of the process, are known to be stable over geological time periods (millions of years). For this reason, mineral sequestration ensures permanent fixation rather than temporary storage of CO₂ guaranteeing no legacy issues for future generations. Readily accessible deposits of magnesium silicate minerals exist as ultramafic complexes along the eastern and western coastal regions of North America (2,3). Globally, these natural raw materials for binding CO₂ exist in grand quantities. Therefore, readily accessible deposits/outcrops exist worldwide in quantities that far exceed even the most optimistic estimates of coal reserves. Finally, the overall mineral carbonation process is exothermic and hence, has the potential to become economically feasible.

The aim of DOE's Mineral Carbonation Program is to generate a valuable knowledge base that can lead to development of cost-competitive mineral CO₂ sequestration methods. In achieving this goal, mechanisms, kinetics, and heat requirements of various CO₂ mineral reactions must be understood well enough to identify feasible reaction pathways and to permit engineering process development. A secondary and equally significant target is to acquire knowledge essential to understanding the reactions of CO₂ with underground minerals, in support of the U.S. DOE's geological sequestration programs where CO₂ may be injected into deep saline formations, or depleted oil or gas reservoirs. Knowledge of the reaction characteristics of CO₂ with various minerals at elevated pressures and temperatures such as those found deep underground would help predict the long-term effects of such practices.

Experiments investigating the reactivities of olivine and serpentine in aqueous and bicarbonate aqueous solutions under supercritical CO₂ pressures were conducted to help determine effects of particle size, P_{CO2}, temperature, and solution chemistry. Here we summarize published continuous-stirred-tank-reactor (CSTR) results (4,5) for reactions of ultramafic minerals with supercritical CO₂ and, for comparison, with a lignite fly ash.

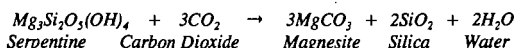
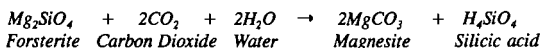
MATERIALS AND METHODS

All mineral carbonation reactions were performed in Hastelloy C-276 autoclaves. Tests were conducted at subcritical (P_{CO2} = 51 atmospheres) and supercritical CO₂ (P_{CO2} = 80, 126, and 136 atmospheres) pressures; reaction temperatures of 155°, 185°, and 230°C and residence times ranging from 3 to 144 hours. In a typical experiment, finely ground minerals and water (15-20% solids concentration) were charged into the CSTR. The CSTR was immediately sealed, purged with

gaseous CO₂, weighed (tare weight), and submerged into an ice bath. Liquid CO₂ was carefully injected through the side port of the autoclave while heating to a pre-calculated process temperature and pressure. The mineral/water/liquid CO₂ mixture was sufficiently agitated during heat up to prevent any settling of magnesium-enriched solids. A modified CSTR system to include a CO₂ gas booster pump and pressure switch was latter designed and operated under relatively constant CO₂ pressures. The addition of the gas booster pump permitted successful operation at an operating pressure of 126 atmospheres (P_{CO2} = 115 atmospheres).

RESULTS & DISCUSSION

The conceptual process for sequestering CO₂ as mineral carbonates was initially proposed by O'Connor, et. al. (4,5) utilizing olivine, water, and supercritical carbon dioxide. In this method, injected CO₂ is dissolved in a slurry of water and mineral reactant, such as olivine. The CO₂ reacts with the olivine/water mixture forming carbonic acid, which dissociates into hydrogen cations and bicarbonate anions. Reaction of carbonic acid with the solid mineral consumes most of the hydrogen cations and liberates equivalent amounts of magnesium cations. These Mg²⁺ cations react with the HCO₃⁻ to form magnesite (MgCO₃). Under supercritical CO₂ pressures, carbonic acid is continuously being generated, consumed, and regenerated. The reaction sequence is concluded: 1) when the reactive surface of the mineral particle is depleted or 2) becomes inactive by mass transfer resistance (i.e., formation of a foreign oxide coating on the surface of mineral reactant particle). The acid-base chemistry for Mg₂SiO₄ and Mg₃Si₂O₅(OH)₄ are given below:



Olivine [forsterite end member (Mg₂SiO₄)] and serpentine [Mg₃Si₂O₅(OH)₄] were identified as being solid mineral reactants for the direct carbonation reaction (4-7). A foundry-grade olivine (identified as ARC olivine), a natural olivine (Twin Sisters, Washington purchased from WARD'S Natural Science Establishment, Inc.) and a synthetic forsterite sample (Alfa Aesar, a Johnston Matthey Company) were selected based on their desired characteristics of high purity, high MgO concentration and low water content. Chemical analyses of the ARC and WARD'S natural olivine, synthetic forsterite, and Cedar Hills quarry serpentine feed samples are included in Table 1. The magnesium oxide concentration was noticeably higher in the synthetic feed material (57.8 wt %) in comparison to both the ARC olivine (49.7 wt %) and WARD'S olivine samples (51.8 wt %). The basis for the lower MgO concentration in these natural feed minerals was attributed to iron substitution for magnesium within the solid solution series. X-ray diffraction data and patterns identified forsterite (Mg₂SiO₄) as the primary phase for both natural olivine feed samples. XRD also confirmed a trace constituent, enstatite (MgSiO₃), for each of the natural olivine samples. This finding was fully anticipated for the raw materials.

Olivine carbonation results from the preliminary series of tests performed at ARC are included in Table 2. Initial results revealed the mineral carbonation reaction is extremely slow at ambient temperatures and pressures. For example, test MC-14 conducted at 150°C and 750 psi (P_{CO2} = 51 atms.) resulted in only a 17.6% conversion of olivine to magnesite after 144 hours. However, increasing both process temperature and CO₂ partial pressure helped to improve upon the kinetics of the carbonation reaction. This was demonstrated during the series of tests at different time intervals (3, 6, 12, 24, and 48 hours) under identical conditions (T = 185°C and P_{CO2} = 115 atmospheres in distilled water) using again the ARC olivine feed sample. Collectively, carbonation tests conducted within the series under relatively short reaction times (3, 6, and 12 hours) gave minor to moderate conversions of Mg₂SiO₄ to MgCO₃. Under longer residence times (24 and 48 hours), the conversion of silicate to carbonate increased with time-on-stream, achieving 51.8% and 56.1% of its stoichiometric maximum in 24 hours and 48 hours respectively. In substituting the synthetic forsterite for the solid reactant, olivine, within the series, significant improvement in terms of carbonation activity was attained. As shown in Table 2, the synthetic forsterite (MC-3) achieved carbonation to 76% of its stoichiometric maximum in just 3 hours, again at 185°C and 1,850 psig. While the chemical analysis of the synthetic material confirmed nearly exact molar concentrations of MgO and SiO₂ as compared to the natural counterparts, the presence of free periclase (MgO) and its subsequent reactivity with carbonic acid resulted in accelerating the mineral carbonation activity within the CSTR. A series of leach tests were later performed to help quantify the free MgO concentration present in the synthetic forsterite material. Results estimated the synthetic material to contain approximately 11 wt % MgO. Although preliminary in nature, these results tend to suggest MgO acts as a promoting agent within the carbonation reaction.

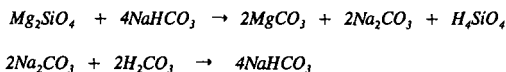
Duplicate experiments at NETL at higher process temperature and pressure (T = 230°C, P_{CO2} = 120 atm in distilled water) conditions coupled with using a minus 325 mesh raw material (WARD'S olivine feed) and a gas dispersion tube within the CSTR provided new evidence into the efficiency of the mineral carbonation reaction. Duplicate CO₂ analysis showed 28.9 weight percent of the recovered solid product as being identified as magnesium carbonate. The extent of reaction was experimentally determined to be over 80% of its stoichiometric maximum after 24 hours.

A major limitation of the CSTR mineral carbonation units at ARC and NETL was its lack of ability to introduce additional CO₂ to the reaction vessel as the carbonation reaction progressed. Hence, for longer test times, the P_{CO₂} decreased with increased extent of reaction, which perhaps retarded the reaction. A modified CTSR system to include a CO₂ gas booster pump and pressure switch was designed and operated at ARC at a operating pressure of 126 atmospheres. This development lead to a major improvement in rate and extent of reaction, as illustrated by the olivine and serpentine carbonation tests shown in tables 2 and 3 respectively. Under the modified system, test MC-25 showed a 91.5% rate of conversion for a finely ground olivine (-325 mesh) mineral to MgCO₃. In view of this finding, the effects of particle size, temperature, and P_{CO₂} on the olivine carbonation reaction were systematically examined.

Particle size of the silicate mineral was recognized as a key element in aiding the acceleration of the mineral dissolution reaction. This effect can be easily viewed by comparing % conversions of tests MC-4, MC-25, and MC-31 shown in Table 2. Under test conditions (T = 185°C, P_{CO₂} = 115 atm. in distilled water), test MC-25 produced over a 90% conversion of Mg₂SiO₄ to MgCO₃ employing a minus 37 micron natural olivine feed. In contrast, tests MC-31 and MC-4 achieved mineral carbonation conversions of 10.6% and 51.8% respectively in 24 hours utilizing the identical feed ARC olivine with the exception of the feed particles sizes being 150 x 106 microns for test MC-31 and 106 x 75 microns for test MC-4.

Another series of completed experiments aided in defining the temperature and CO₂ partial pressure requirements for the olivine carbonation reaction. At 115°C and P_{CO₂} = 80 atmospheres, test MC-42 showed no reaction had occurred after 6 hours. However, significant conversion to carbonate (68.2%) resulted in test MC-43 by increasing the process temperature to 185°C while holding CO₂ pressure identical to that in test MC-42. The extent of reaction, as exemplified in test MC-40, was enhanced further to ~85% by increasing the CO₂ process pressure to 115 atmospheres while holding the process temperature constant.

An improvement in mineral carbonation efficiency was established in modifying the solution chemistry of the liquid reactant, water. The final series of tests was conducted in a bicarbonate aqueous solution, 0.5 M NaHCO₃, 1 M NaCl, which dramatically enhanced the overall reaction rate. Sodium bicarbonate was established as a more effective CO₂ carrier, generating product solutions of nearly 20g/liter CO₂, compared to 0.5-1.0 g/liter CO₂ in tests using distilled water. The modified solution was found to be very stable, with nearly constant pre- and post-test pH values (~7.8), and relatively constant CO₂ concentrations. The following equations represent a possible reaction sequence in the bicarbonate aqueous solution.



NaHCO₃ is consumed by the mineral silicate, along with being regenerated by reaction with carbonic acid, which is also continuously regenerated due to the high P_{CO₂} in the system.

A Cedar Hills serpentine sample obtained from the Pennsylvania/Maryland state line district was selected for serpentine carbonation testing. XRD determinations established antigorite as the primary constituent for the serpentine feed sample with minor elements of chrysotile, magnetite, and kaolinite. Initial carbonation tests (T = 185°C, and P_{CO₂} = 115 atms.) performed for 24 hours with serpentine resulted in a much lower extent of reaction (34%) compared with identical tests conducted with the ARC olivine feed (51%). The removal of (both physically adsorption and chemically bound) inherent water present in the serpentine feed sample via heat treatment was envisioned to produce a more reactive sample. Thermogravimetric analysis (TG) and differential thermal analysis (DTA) were completed on the Cedar Hills feed sample to determine treatment temperature(s). DTA revealed three separate points of inflection, occurring at 160°C, 375°C (evolution of water of crystallization); and 614°C (evolution of constitutional water). For that reason, heat pretreatments were performed at 650°C for 2 hours.

It was also acknowledged that oxidation of the minor constituent magnetite present in the serpentine feed sample during heat treatment could potentially form a passive layer of hematite on the mineral surface, inhibiting the carbonation reaction. Thus, heat treatments on the serpentine feed sample were conducted in both air and CO₂. Chemical analysis of the air-treated products identified hematite being present, while magnetite oxidation to hematite was limited during treatments in CO₂. XRD analysis also confirms heat-treated serpentine samples were partially transformed to forsterite.

Table 3 shows both the serpentine carbonation conditions and results obtained in the series of tests performed at ARC. Tests conducted in distilled water for 24 hours showed marginal improvement in the serpentine carbonation reaction with the air-treated sample (57%) in comparison to the untreated serpentine sample (34%). Test MC-37 utilizing an air-treated serpentine feed sample showed a moderate improvement in extent of reaction (63.5%) for the serpentine carbonation test conducted in a bicarbonate aqueous solution (0.5 M NaHCO₃). The effect of gaseous atmosphere (CO₂ versus air) during heat treatments of serpentine was found significant for the carbonation tests conducted in the carbonation starting solution, 0.5 M NaHCO₃, 1 M NaCl. Extent of reaction increased to over 83% for the serpentine heat-treated in CO₂ compared to 41% for the serpentine treated in air. Both results were achieved in identical carbonation tests (T = 185°C; P_{CO₂} = 115 atms) conducted for 6 hours. In contrast, test MC-44 conducted under identical conditions utilizing

an untreated serpentine feed sample showed only minor conversion of serpentine to magnesite (6.8%) after 6 hours.

Finally, studies at NETL demonstrated a lignite fly ash (16% CaO + MgO) could also be used to produce a carbonated product as identified by XRD. Recent work by Anthony et. al. (8) has shown carbonation to be rapid at FBC operating conditions for dry ashes above 400°C. Hydration of the ash promotes the carbonation reaction below this temperature. Fly ash is seen as an excellent candidate to be used solely or in conjunction with mineral silicates for sequestering CO₂ within the mineral carbonation process. Future work at NETL will utilize a Coal Combustion By-product (CCB) database system for identifying best candidates to be used in the Mineral Carbonation Study Program.

CONCLUSIONS

DOE-sponsored carbon sequestration research at NETL, ARC, LANL, and ASU is addressing important issues related to the mineral sequestration of CO₂. Experimental investigations confirm magnesium silicates, olivine and serpentine, are equally amenable to the mineral carbonation process, even though serpentine requires heat treatment. Experimental data are being sought to help facilitate and develop kinetic models that can be employed to identify large-scale, cost-effective mineral sequestration strategies and to evaluate its physical, chemical, and environmental effects on the terrestrial and underground environments.

DISCLAIMER

Reference in this report to any specific product, process, or service is to facilitate understanding and does not imply its endorsement or favoring by the United States Department of Energy.

REFERENCES

1. Freund, P., and Ormerod, W.G. "Progress Toward Storage of Carbon Dioxide." Energy Conversion Management #8:S199; 1997
2. Goff, F.; Guthrie, G.; Counce, D.; Kluk, E.; Bergfeld, D.; and Snow, M. Preliminary Investigations on the Carbon Dioxide Sequestering Potential of Ultramafic Rocks. Los Alamos, New Mexico: Los Alamos National Laboratory; LA-13328-MS; 1997, 22 pp.
3. Hunter, C.E. Forsterite Olivine Deposits of North Carolina and Georgia. Raleigh, North Carolina: North Carolina Department of Conservation and Development; Bulletin 41; 1941, 117 pp.
4. O' Connor, W.K., Dahlin, D. C., Walters, R. P., and Turner, P. C., "Carbon Dioxide Sequestration by Ex-Situ Mineral Carbonation," Proceedings, Second Annual Dixy Lee Ray Symposium, American Society of Mechanical Engineers, Washington, D.C., August 29-September 2, 1999
5. O' Connor, W.K., Dahlin, D. C., Nilsen, D. N., Walters, R. P., and "Carbon Dioxide Sequestration by Direct Mineral Carbonation with Carbonic Acid," Proceedings, 25th International Technical Conference on Coal Utilization and Fuel Systems, Coal Technology Association, Clearwater, Florida, March 6-9, 2000
6. Lackner, K. S., Butt, D. P., Wendt, C. H., and Sharp, D. H. "Carbon Dioxide Disposal in Solid Form", Proceedings of 21st International Conference on Coal Utilization and Fuel Systems, Coal Technology Association, Clearwater, FL; 1996
7. Lackner, K. S., Wendt, C. H., Butt, D. P., Joyce, E. L., and Sharp, D. H. "Carbon Dioxide Disposal in Carbonate Minerals", Energy, Vol. 20, No. 11, pp 1153-1170, 1995
8. Anthony, E.J.; et.al., "Pacification of high calcic residues using carbon dioxide", Waste Management, Vol 20, Issue 1, Feb. 2000

Table 1. Chemical composition of reactant minerals, wt %

Oxide	ARC Olivine	WARD'S Olivine	Alfa Aesar Forsterite	Cedar Hills serpentine
Al ₂ O ₃	0.208	0.148	0.264	0.156
CaO	0.070	0.130	0.661	0.028
Cr ₂ O ₃	0.044	N/A	0.012	0.037
FeO	5.966	N/A	0.009	4.333
Fe ₂ O ₃	2.558	9.059	0.000	2.629
MgO	49.677	51.789	57.845	45.843
K ₂ O	0.007	0.02	0.019	<0.002
SiO ₂	41.357	38.205	37.929	37.500
Na ₂ O	0.099	0.00	0.101	<0.002
Volatiles ¹	0.401	0.70	0.123	11.500
Total	100.387	100.051	96.963	102.026

¹ Volatile constituents include: fixed carbon, mineral carbon, water

N/A - not available

Table 2 – Olivine Carbonation Tests – Test Summary

Test	Particle size, microns	Time, Hrs	Temp., C	PCO ₂ , atm	Carbonation Starting Solution	Product Solids- CO ₂ , wt pct	Percent Stoichiometric Conversion
MC-3	-44	3	185	115	Distilled H ₂ O	32.50	76.0
MC-4	106 x 75	24	185	115	Distilled H ₂ O	18.30	51.8
MC-10	53 x 37	6	185	115	Distilled H ₂ O	1.25	3.5
MC-11	53 x 37	48	185	115	Distilled H ₂ O	19.80	56.1
MC-12	53 x 37	3	185	115	Distilled H ₂ O	0.33	0.9
MC-13	53 x 37	12	185	115	Distilled H ₂ O	6.58	18.6
MC-14	53 x 37	144	150	51	Distilled H ₂ O	6.21	17.6
MC-25 ¹	-37	24	185	115	Distilled H ₂ O	32.30	91.5
MC-31	150 x 106	24	185	115	Distilled H ₂ O	3.74	10.6
MC-40	-37	6	185	115	0.5 M NaHCO ₃ , 1 M NaCl	29.80	84.4
MC-42	-37	6	115	80	0.5 M NaHCO ₃ , 1 M NaCl	0.00	0.0
MC-43	-37	6	185	80	0.5 M NaHCO ₃ , 1 M NaCl	24.09	68.2

¹ Test MC-25 and all subsequent tests conducted in modified CSTR facility with gas dispersion

Table 3 – Serpentine Carbonation Tests – Test Summary

Test	Particle Size microns	Heat Pretreatment ¹	Time, Hrs	Temperature	PCO ₂ atmospheres	Carbonation Starting Solution	Product Solids CO ₂ , wt pct	Percent Stoichiometric Conversion
MC-32	-37		24	185	115	Distilled H ₂ O	11.40	34.2
MC-33	-37		24	185	115	Distilled H ₂ O	11.50	34.5
MC-34	-37	in air	24	185	115	Distilled H ₂ O	22.30	57.0
MC-37	-37	in air	24	185	115	0.5 M NaHCO ₃	22.60	63.5
MC-38	-37	in air	24	185	115	0.5 M NaHCO ₃ , 1 M NaCl	24.70	69.4
MC-39	-37	in CO ₂	6	185	115	0.5 M NaHCO ₃ , 1 M NaCl	28.20	83.2
MC-41	-37	in CO ₂	24	185	115	Distilled H ₂ O	20.17	59.5
MC-44	-37	in air	6	185	115	0.5 M NaHCO ₃ , 1 M NaCl	2.28	6.8
MC-45	-37	in air	6	185	115	0.5 M NaHCO ₃ , 1 M NaCl	14.45	40.6

¹ Heat treatments conducted for 2 hours at 600-650°C

DEVELOPMENT OF INTEGRATED SYSTEM FOR BIOMIMETIC CO₂ SEQUESTRATION USING THE ENZYME CARBONIC ANHYDRASE

Gillian M. Bond¹, John Stringer², Donald K. Brandvold³, F. Arzum Simsek¹, Margaret-Gail Medina¹, and Gerald Egeland¹

¹Department of Materials & Metallurgical Engineering, New Mexico Tech, Socorro, NM 87801

²Electric Power Research Institute, 3412 Hillview Avenue, Palo Alto, CA 94304

³Department of Chemistry, New Mexico Tech, Socorro, NM 87801

KEYWORDS: CO₂ sequestration, biomimetic, enzyme

INTRODUCTION

Many possible approaches to carbon sequestration are being investigated by researchers worldwide (see, e.g., Bond et al., 1999 a, b; Department of Energy, 1997; Hendriks, 1994; Herzog, 1997; Knotek and Eisenberger, 1998; Lackner et al., 1995; Yamada, 1998). This is good, because the scale of anthropogenic CO₂ emissions is so huge that sequestration of anything more than a small fraction of it is likely to require a combination of different approaches. Most sequestration studies have been based on the assumption that CO₂ would first have to be separated from the remainder of the exhaust gases from fossil-fuel combustion. It could then be disposed of, for example, in DOG (depleted oil and gas) wells, in deep saline aquifers, in the deep ocean, or through deposition into minerals such as peridotites or serpentinites. A common theme for all of these approaches is that they involve the need to concentrate and, for the most part, transport CO₂. However, whilst it is technically feasible to remove CO₂ from flue gases with existing technology (Hendriks, 1994; Yamada, 1998), the removal systems require large amounts of capital and energy, and could raise the cost of busbar electricity, for example, by 50% (Department of Energy, 1997). Transportation of CO₂ by pipeline as a supercritical fluid is a well-established technology in EOR (enhanced oil recovery), but still is not cheap.

Our present research is aimed at the development of a novel biomimetic approach to CO₂ sequestration. The intent is to develop a CO₂ scrubber that can be used to reduce CO₂ emissions from, for example, fossil-fuel-burning power plants, based on the use of an enzyme or biological catalyst. The resulting sequestration system would offer several potential advantages, including: a plant-by-plant solution to emission reduction; no costly CO₂ concentration and transportation steps; a safe, stable, environmentally benign product; and an environmentally benign process. Proof of principle has already been demonstrated (Bond et al., 1999 a, b). The present emphasis will be on the performance of the enzyme in the presence of other chemical species likely to be present in the industrial situation. It is useful first, however, to summarize the biomimetic approach, in order to put the present results in context.

Atmospheric levels of CO₂ are much lower today than they were early in the earth's history. Carbonate minerals, such as calcite, aragonite, dolomite, and dolomitic limestone, comprise a massive CO₂ reservoir, estimated (Wright et al., 1995) to contain an amount of carbon equivalent to 150,000 x 10¹² metric tons of CO₂. Thus carbonate minerals offer a geologically proven, safe, long-term repository for CO₂. If anthropogenic CO₂ can be fixed into solid carbonate form, such as calcium carbonate, then we have a stable and environmentally friendly product. The problem, of course, is one of rate.

In order to address the problem of rate, we adopted a biomimetic approach (Bond et al., 1999 a, b). It is useful to keep in mind here that we are defining a biomimetic approach as one in which a particular aspect of a biological process or structure is identified and applied to solve a specific non-biological problem (Bond et al., 1999 a). In other words, it is an approach in which:

- We have a specific engineering problem to solve.
- We identify a biological system in which an analogous engineering problem has been solved.
- We use the enabling part of that system, whether it be a structural design, a processing route, or a biochemical component, to solve our engineering problem.

In the present instance, we examined the rate-limiting step in the chemistry of CO₂ fixation into calcium carbonate in aqueous solution, and then considered what lessons could be learned from biological systems in order to accelerate that step. Calcium carbonate precipitates readily from aqueous solution given a suitable saturation of calcium and carbonate ions, and so the issue becomes one of how to produce carbonate ions rapidly from CO₂ and H₂O (Wilbur and Simkiss, 1968). One important parameter to be considered is pH, because of its strong effect on the proportions of the carbonic species present (Loewenthal and Marais, 1978), and because, at low pH, carbonates will tend to dissolve rather than precipitate. Although carbonate could be formed rapidly at high pH, this would pose both economic and environmental concerns, and hence a

process that operates at very mildly basic pH values would be desirable. Gaseous CO₂ dissolves rapidly in water, producing a loosely hydrated aqueous form (Quinn and Jones, 1936; Keene, 1993). Three additional reactions are then required to form carbonate ions at moderate pH:

- Hydration of aqueous CO₂ to produce carbonic acid (H₂CO₃).
- Dissociation of carbonic acid into bicarbonate ions and protons.
- Production of carbonate ions from bicarbonate ions.

By far the slowest of these reactions is the hydration of CO₂ (Keene, 1993).

A solution to the problem of accelerated CO₂ hydration, in fact, already exists in biological systems. The carbonic anhydrases (CAs) are a broad group of zinc metalloenzymes that are ubiquitous in nature (Brown, 1990; Dodgson et al., 1991; Pocker, 1990). They are among the fastest enzymes known, and they catalyze the reversible hydration of CO₂. The fastest CA isozyme known is the human isozyme HCA II, each molecule of which can hydrate at least 1.4×10^6 molecules of CO₂ per second (Khalifah and Silverman, 1991); the catalyzed hydration occurs at or near the diffusion-controlled limit for the encounter rate of enzyme and CO₂. Thus, if we use CA to catalyze the hydration of CO₂, it should be possible to fix large quantities of CO₂ into carbonate form, without recourse to caustic conditions. [Another group has, in fact, been looking at CA as a catalyst for short-term aqueous sequestration of CO₂ for use in completely closed systems, such as a space station (M. Trachtenberg, personal communication).]

Feasibility of our biomimetic approach was demonstrated (Bond et al., 1999 a, b), based on two types of experiment. One was designed to show acceleration of the overall process of forming a solid product (calcium carbonate) in the presence of CA. This involves a series of steps beyond the hydration of CO₂, but is vital to show potential industrial applicability. The other was designed to demonstrate the accelerated hydration of CO₂ in the presence of CA. This shows catalysis of a single reaction, and hence is applicable also to comparisons of enzyme performance for different isozymes, and under different conditions. Following the successful proof of principle, several topics were identified as needing further study, and some of these are discussed in Bond et al. (1999 a, b). One of these topics is optimization of the catalyst. The activity and lifetime of the enzyme will be influenced by a range of factors, including pH, temperature, and other ions present. The ions present will depend on the source of the water used (seawater or freshwater), as well as on the other species present in the flue gases.

Some inhibition of CA activity by various anions has been reported previously (see, e.g., Maren et al., 1976 [Δ pH]; Pocker and Stone, 1967 [*p*-NPA assay]). By the far the most potent of the inorganic anionic inhibitors of CA, however, is CN⁻, which is not an issue for the proposed application. Very small amounts (unlikely to exceed 100 ppm) of SO_x (Electric Power Research Institute, 1984) and NO_x may be present in the flue gases. Higher concentrations of anions are likely in the water used, particularly, of course, if it is seawater.

EXPERIMENTAL

A suitable catalyst (or isozyme) for an industrial-scale CO₂ scrubber will have to be fast, robust, and capable of being produced in large amounts cost effectively. The simplest and cheapest means of obtaining large amounts of CA will be by means of overexpression by a genetically modified bacterial system, and we are working with two different isozymes for which other research groups have successfully cloned genes. In the short term, however, initial experiments on anionic inhibition have been performed on BCA (bovine erythrocyte CA), purchased in purified form from Sigma Chemical Corporation.

The method that has been used to show the accelerated hydration of CO₂ is a Δ pH method (Henry, 1991). CA catalyzes the reversible hydration reaction between CO₂ and H₂O, producing HCO₃⁻ and H⁺. This production of protons leads to a change in pH as the reaction proceeds towards equilibrium. Measurement of this pH change as a function of time forms the basis of the Δ pH method. Measurements are usually made at temperatures in the range 0-5°C, to slow the enzyme-catalyzed reaction which is otherwise so rapid that initial rates are hard to measure (Henry, 1991). A World Precision Instruments Bee-Trode pH electrode and Dri-Ref system, with an ATC (automatic temperature compensation) probe, connected to an Orion Sensorlink pH data acquisition system, was used for temperature-compensated pH monitoring. Activities were measured and compared for 30 μ g/ml BCA in 2.5 mM aqueous CO₂ solution, in the presence of different concentrations of Na₂SO₄ and NaNO₃, in 25 mM pH 7.4 tris buffer, at 1-3 °C. CA activity in ASW-based solution (artificial seawater) was also compared to that in deionized-water-based solution. ASW was produced by dissolution of Sigma artificial-seawater salts, 38g of which were added to 1 liter of deionized water prior to bubbling with CO₂. In this case, the weak buffering was achieved with Barbitol buffer.

A *p*-NPA assay has also been used to monitor the activity of CA, based on the enzyme-mediated hydrolysis of para-nitrophenyl acetate (Pocker and Stone, 1967). The same enzyme active site that is responsible for acceleration of CO₂ hydration also accelerates this hydrolysis reaction, which yields a bright yellow product that absorbs at 405 nm and can be determined spectrophotometrically. Due to steric factors, however, the reaction rate is much slower for the hydrolysis reaction than for the hydration of CO₂. Thus the enzyme-accelerated hydrolysis rates can be conveniently monitored without cooling (in contrast to the delta pH measurements of accelerated CO₂ hydration), making the *p*-NPA assay useful for a first look at the influence of different parameters on CA activity. Activities were measured and compared for 20 μg/ml BCA in the presence of different concentrations of Na₂SO₄ and NaNO₃, in 50 mM pH 7.4 tris buffer, at 25°C. Stock solutions of 0.0025g/ml *p*-NPA were prepared in acetonitrile, which was used to prevent spontaneous decomposition of *p*-NPA in air or in water. 10% (v/v) was added into each sample solution. The absorbance intensity at 405 nm for the yellow product, *p*-nitrophenol, was followed versus time with a Hitachi-330 spectrophotometer. The slope of absorbance versus time was defined as the activity gradient.

RESULTS

Absorbance-versus-time plots from the *p*-NPA assay are shown for SO₄²⁻ concentrations ranging from 0.5 mM up to 200 mM in Figure 1. There is little inhibition at concentrations up to 5 mM (480 ppm), but there is significant inhibition by 50 mM. Similar plots are shown for NO₃⁻, again over a concentration range of 0.5 mM up to 200 mM, in Figure 2. Again, large-scale inhibition starts somewhere between 5 mM (310 ppm) and 50 mM.

Delta pH data for different SO₄²⁻ and NO₃⁻ concentrations, ranging from 5 mM to 200 mM, are shown in Figures 3 and 4 respectively. There is little indication of inhibition at concentrations below 100-200 mM. Figure 5 shows a comparison of enzyme activity in ASW-based solution versus DI-water-based solution. The enzyme is seen to perform well in both solutions.

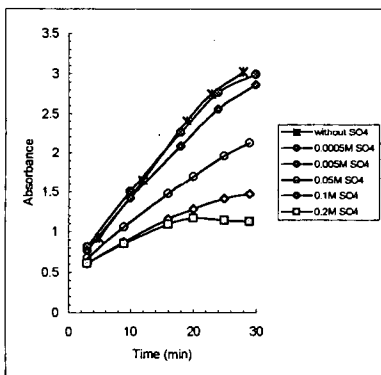


Figure 1. *p*-NPA activity of BCA in various concentrations of SO_x, in tris buffer.

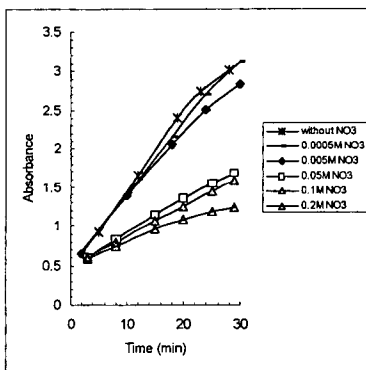


Figure 2. *p*-NPA activity of BCA in various concentrations of NO_x, in tris buffer.

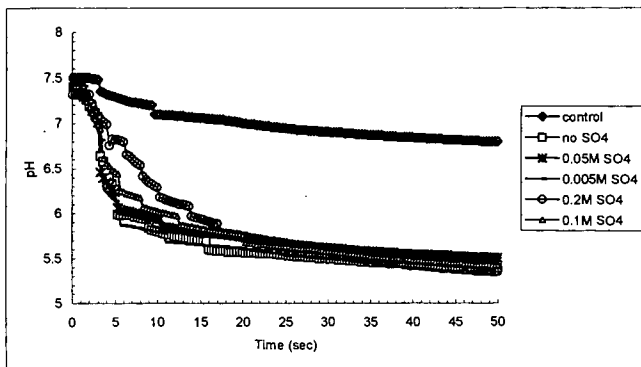


Figure 3. Delta-pH activity of BCA in various concentrations of SO_x, in tris buffer.

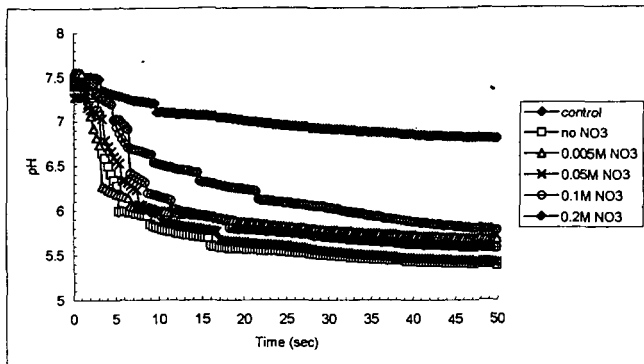


Figure 4. Delta-pH activity of BCA in various concentrations of NO_x , in tris buffer.

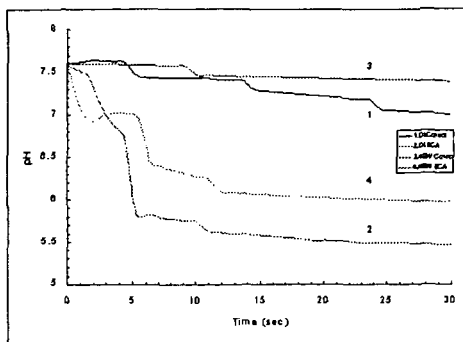


Figure 5. Delta-pH activity of BCA in artificial seawater (ASW) and de-ionized water (DI) tested in barbital buffer.

DISCUSSION

It is interesting to note that the enzyme appears to be less susceptible to inhibition as determined by the delta pH technique, than by the *p*-NPA assay. It should be remembered, however, that the enzyme is also a much less efficient catalyst for the hydrolysis of *p*-NPA than it is for the hydration of CO_2 , and hence it is perhaps not surprising that that already somewhat difficult catalytic action should be more easily inhibited. It is clear that, for the present purposes of catalyst optimization, the *p*-NPA assay has a useful role to play for convenient initial screening, but the final assay should be delta pH.

Given the low levels of SO_x and NO_x that would be present in flue gases reaching a CO_2 scrubber located behind a sulfur scrubber, it appears very unlikely that either of these species would present an inhibition problem to the enzyme in such a system. It also appears unlikely that the type of water used will pose an inhibition problem, even for seawater, as represented here by the ASW-based solution. Similar experiments will be performed on the other isozymes, produced by bacterial overexpression, that we are currently investigating.

CONCLUSIONS

The enzyme, carbonic anhydrase, is the biological catalyst responsible for the interconversion of CO_2 and bicarbonate in living organisms. The present research is aimed at the development of a CO_2 scrubber that can be used to reduce CO_2 emissions from, for example, fossil-fuel-burning power plants. In this system, the enzyme works as a catalyst to accelerate the rate of CO_2 hydration for subsequent fixation into stable mineral carbonates, the counterions for which may be supplied from such sources as waste brines from desalination operations. Proof of principle has already been demonstrated. One of the requirements for the enzyme will be that it must be able to function in the presence of other chemical species likely to be present in the industrial application. The present results show excellent enzyme activity in the presence of low levels of SO_x and NO_x (that might be expected from flue gases) and also in solution representative of seawater.

ACKNOWLEDGMENT

The authors gratefully acknowledge support from EPRI under contract number WO9000-26.

REFERENCES

- Bond, G.M., G. Egeland, D.K. Brandvold, M.G. Medina and J. Stringer, pp. 763-781, in Mishra, B., editor, *EPD Congress*, TMS, Warrendale, (1999 a).
- Bond, G.M. G. Egeland, D.K. Brandvold, M.G. Medina, F.A. Simsek, and J. Stringer, *World Resource Review*, **11**, 603 (1999 b).
- Brown, R.S., pp. 145-180, in Aresta, M. and J.V. Schloss, editors, *Enzymatic and Model Carboxylation and Reduction Reactions for Carbon Dioxide Utilization*, NATO ASI Series, Series C: Mathematical and Physical Sciences, vol. 314, Kluwer Academic Publishers, Dordrecht (1990).
- Department of Energy (Office of Energy Research), *Carbon Management: Assessment of Fundamental Research Needs*, DOE, Washington, (1997).
- Electric Power Research Institute, *Field Investigation of FGD System Chemistry*, EPRI CS-3796 (12/1984).
- Dodgson, S.J., R.E. Tashian, G. Gros and N.D. Carter, editors, *The Carbonic Anhydrases: Cellular Physiology and Molecular Genetics*, Plenum Press, New York (1991).
- Hendriks, C., *Carbon Dioxide Removal from Coal-Fired Power Plants*, Kluwer Academic Publishers, Dordrecht (1994).
- Herzog, H.J., editor, *Proceedings of the Third International Conference on Carbon Dioxide Removal, Energy Conversion and Management*, **38 Suppl.** (1997).
- Keene, F.R., pp. 1-18, in Sullivan, B.P., K. Krist and H.E. Guard, editors, *Electrochemical and Electrocatalytic Reactions of Carbon Dioxide*, Elsevier, Amsterdam (1993).
- Khalifah, R.G. and D.N. Silverman, pp. 49-70, in Dodgson, S.J., R.E. Tashian, G. Gros and N.D. Carter, editors, *The Carbonic Anhydrases: Cellular Physiology and Molecular Genetics*, Plenum Press, New York (1991).
- Knotek, M. and P. Eisenberger, co-chairs, *Basic Research Needs to Attain Sustainability: The Carbon Problem*, Workshop held at Tucson, AZ (October 1998).
- Lackner, K.S., C.H. Wendt, D.P. Butt, E.L. Joyce and D.H. Sharp, *Energy*, **20**, 1153 (1995).
- Loewenthal, R.E. and G.v.R. Marais, *Carbonate Chemistry of Aquatic Systems: Theory and Application*, volume 1, chapter 3, Ann Arbor Science, Ann Arbor (second printing, 1978).
- Maren, T.H., C.S. Rayburn, and N.E. Liddell, *Science*, **191**, 469 (1976).
- Pocker, Y., pp. 129-143, in Aresta, M. and J.V. Schloss, editors, *Enzymatic and Model Carboxylation and Reduction Reactions for Carbon Dioxide Utilization*, NATO ASI Series, Series C: Mathematical and Physical Sciences, vol. 314, Kluwer Academic Publishers, Dordrecht (1990).
- Pocker, Y. and J.T. Stone, *Biochemistry*, **6**, 668 (1967).
- Quinn, E.L. and C.L. Jones, *Carbon Dioxide*, Reinhold Publishing Corporation, New York (1936).
- Wilbur, K.M. and K. Simkiss, *Comparative Biochemistry*, **26A**, 229 (1968).
- Wright, J., A. Colling and Open University Course Team, *Seawater: Its Composition, Properties and Behaviour*, 2nd Edition, Pergamon-Elsevier, Oxford (1995).
- Yamada, K., pp. 77-86, in Inui, T., M. Anpo, K. Izui, S. Yanagida and T. Yamaguchi, editors, *Advances in Chemical Conversions for Mitigating Carbon Dioxide*, *Studies in Surface Science and Catalysis*, vol. 114, Elsevier, Amsterdam (1998).

Roger C. Dahlman¹ and Gary K. Jacobs²

¹U.S. Department of Energy
Office of Science, Biological and Environmental Research
19901 Germantown Road, MS-F-240
Germantown, MD 20874-1290

²Environmental Sciences Division
Oak Ridge National Laboratory*
P.O. Box 2008
Building 1505, MS-6035
Oak Ridge, TN 37831-6035

ABSTRACT

Carbon sequestration is a growing research topic that addresses one important aspect of an overall strategy for carbon management to help mitigate the increasing emissions of CO₂ into the atmosphere. There are estimates that terrestrial ecosystems could sequester significant quantities of carbon over the next 50 years. The impact of this sequestration could help buy time for other technologies to come on-line by delaying the need for more dramatic decreases in global emissions. There is increasing interest in scientific advances that can be used to further enhance this potential sequestration of carbon in soils. This paper summarizes current research that is addressing some of the major uncertainties in the carbon cycle and introduces new research that is being initiated specifically related to carbon sequestration in terrestrial ecosystems.

KEYWORDS

Carbon sequestration, carbon cycle, climate change, AmeriFlux, ecosystem research, soil carbon

INTRODUCTION

Currently, emissions of CO₂ are increasing globally and are projected to double over the next century. [1] This excess CO₂ enters the global carbon cycle where part remains in the atmosphere, part is taken up by oceans and the terrestrial biosphere. But significant uncertainty still surrounds the quantitative description of the natural carbon cycle. A major challenge of the greenhouse gas and climate change issue is to understand what happens to the excess CO₂ generated from the burning of fossil fuels. In particular, the rate and magnitude by which excess carbon is assimilated into terrestrial and oceanic sinks will determine the balance that remains in the atmosphere. While research in this challenging area continues, there are new efforts to begin research that might help mitigate increasing CO₂ emissions through special efforts to sequester CO₂.

Carbon sequestration in terrestrial ecosystems can be defined as the net removal of CO₂ from the atmosphere into long-lived pools of carbon. The pools can be living, aboveground biomass (e.g., trees), wood products with a long, useful life created from biomass (e.g., lumber), living biomass in soils (e.g., roots and microorganisms), or recalcitrant organic and inorganic carbon in soils and deeper subsurface environments. It is important to emphasize that increasing photosynthetic carbon fixation alone is not enough. This carbon must be fixed into long-lived pools. Otherwise, one may be simply altering the size of fluxes in the carbon cycle, not increasing carbon sequestration.

THE DOE ROADMAP FOR CARBON SEQUESTRATION

The U. S. Department of Energy (DOE) has recently completed a report that details the state of science related to carbon sequestration. [2] The report also lays out future research topics that will be necessary in achieving increases in carbon sequestration. There are four main objectives that must be addressed for terrestrial ecosystems: (1) assessing ecosystem dynamics, (2)

* Oak Ridge National Laboratory is managed by UT-Battelle LLC, for the U.S. Dept. of Energy under contract DE-AC05-00OR22725. The submitted manuscript has been authored by a contractor of the U.S. Government under contract DE-AC05-00OR22725. Accordingly, the U.S. Government retains a nonexclusive, royalty-free license to publish or reproduce the published form of this contribution, or allow others to do so, for U.S. Government purposes.

increasing below-ground carbon stocks, (3) increasing the rate of growth, standing stocks of carbon, and utilization of above-ground biomass, and (4) optimizing land use for carbon sequestration. It is important to remember that while many processes occur at the molecular level (i.e., photosynthesis, formation and protection of soil organic matter, etc), management practices to enhance carbon sequestration will be implemented at the landscape scale. At this scale ecosystems are the key functional units for estimating productivity and carbon sequestration, and for assessing potentially deleterious impacts associated with efforts to increase carbon in ecosystems.

The DOE report goes on to detail examples of specific research areas that are ripe for innovations that will advance our scientific underpinnings for enhanced sequestration. The other key component of research is on developing improved measurement and monitoring systems. It will be important to be able to determine what sequestration methods are working, and current measurement techniques are lacking in sensitivity and spatial resolution. The Offices of Science and Fossil Energy of the U.S. Department of Energy are implementing research opportunities identified by the state of the science report.

CURRENT RESEARCH IN DOE

While the DOE Office of Science/Biological and Environmental Research (OBER) is embarking on a new research program focused on carbon sequestration in terrestrial ecosystems, current research efforts in OBER have been addressing the natural carbon cycle and potential impacts to ecosystems from global change for some time.

The Terrestrial Carbon Program (TCP) performs research that provides the scientific underpinnings for predicting future concentrations of CO₂ in the atmosphere. The research, which focuses on natural systems that regulate the abundance of CO₂ in the atmosphere, emphasizes (i) understanding the processes controlling exchange rate of CO₂ between atmosphere and terrestrial biosphere; (ii) developing process-based models of atmosphere-terrestrial carbon exchange; (iii) evaluating source-sink mechanisms for atmospheric CO₂; and (iv) improving reliability of global carbon models for predicting future atmospheric concentrations of CO₂. Three particularly key parts of the TCP are:

- Mechanistic terrestrial carbon models for evaluating the role of the biosphere in atmospheric CO₂ changes, and the influence of climate and other feedbacks on the biogeochemical cycle of carbon.
- AmeriFlux network of CO₂ measurements for estimating carbon cycling by terrestrial ecosystems.
- Free Air CO₂ Enrichments (FACE) experiments that evaluate the responses of terrestrial plants and ecosystems to increased concentrations of atmospheric CO₂.

AmeriFlux involves the measurement of net CO₂ exchange of representative ecosystems across United States and North America. For the present network of 35 sites, net annual CO₂ exchange is measured by eddy covariance methods producing annual estimates of net carbon gain or loss by ecosystems such as forests, grasslands and croplands. In addition to flux measurements, biological/ecological data are collected on processes such as photosynthesis, respiration, primary productivity and growth rates and the turnover of different ecosystem carbon pools. Together with flux measurements these data provide unique estimates of net ecosystem production (NEP); positive values of NEP mean the system is storing carbon and negative values indicate net loss of carbon. Initial results show that forest ecosystems are gaining carbon at the rate of 2 to 6 tons of carbon per hectare per year. This network of flux measurements, and related ecosystem and micrometeorological data collectively provide vital ground surface information about carbon sequestration. The data also help interpret other observations of atmospheric CO₂ and space-based information about ground surface processes. Research products of AmeriFlux contribute significantly to the understanding of the role of the terrestrial biosphere in the global carbon cycle, to uniquely quantify carbon sequestration by the terrestrial biosphere, and to provide vital data for evaluating the hypothesis that N. America is a significant terrestrial carbon sink.

The Program for Ecosystem Research (PER) includes both experimental and modeling research related to both the direct and indirect effects of climatic and atmospheric changes on ecosystem components and processes. Research emphasizes the detection and quantification of adjustments to global atmospheric and climatic changes (e.g., temperature, moisture, ozone, CO₂) and the

mechanisms that control the observed adjustment processes. Ecosystem responses that are studied include (1) ecological adjustments such as changes in the organized hierarchy of ecosystem processes, structure, and diversity; and (2) biological adjustments at the organism level that are manifested at the ecosystem level, including homeostatic (physiological, biochemical) and genetic responses.

NEW RESEARCH DIRECTIONS

DOE formed a new center in 1999 to focus on research related to enhancing carbon sequestration in terrestrial ecosystems. A consortium of institutions (see next section) will perform research to help determine how to increase the amount of carbon entering into "pools" that are stabilized in soil and protected against decomposition. The center will also research ways to measure, monitor and verify sequestration so that it may be appropriately accounted for in national inventories of greenhouse gas emissions.

In addition to the Centers approach, there is a solicitation for research from the scientific community involving investigator-initiated ideas and innovative research for enhancing carbon sequestration of terrestrial ecosystems. New ideas and concepts will be selected from the competition that can be expected to promote significantly increased capture and storage of carbon by terrestrial ecosystems.

THE DOE CENTER FOR RESEARCH TO ENHANCE CARBON SEQUESTRATION IN TERRESTRIAL ECOSYSTEMS (CSiTE)

The newly formed research center is known as CSiTE – Carbon Sequestration in Terrestrial Ecosystems. CSiTE performs fundamental research that supports methods that will lead to enhanced carbon sequestration in terrestrial ecosystems as one component of a carbon management strategy. The goal of CSiTE is to discover and characterize links between critical pathways and mechanisms for creating larger, longer-lasting carbon pools in terrestrial ecosystems. Research is designed to establish the scientific basis for enhancing carbon capture and long-term sequestration in terrestrial ecosystems by developing (1) scientific understanding of carbon capture and sequestration mechanisms in terrestrial ecosystems across multiple scales from the molecular to the landscape, (2) conceptual and simulation models for extrapolation of process understanding across spatial and temporal scales, (3) estimates of national carbon sequestration potential, and (4) assessments of environmental impacts and economic implications of carbon sequestration.

SUMMARY

Carbon sequestration is an important part of an overall carbon management strategy to help reduce and/or mitigate global CO₂ emissions. Research into how to enhance sequestration in terrestrial ecosystems could lead to significant beneficial practices that could be implemented during the next 20-50 years. These practices could help "buy time" for other methods of sequestration and energy technologies to come on-line. At the same time, it is essential to continue to emphasize understanding the carbon cycle which drives future global change scenarios and also can impact the efficacy of sequestration options in natural systems.

ACKNOWLEDGMENTS

Research sponsored by the U.S. Department of Energy, Office of Science, Biological and Environmental Research. This paper is a contribution from CSiTE – The Center for Research to Enhance Carbon Sequestration In Terrestrial Ecosystems.

REFERENCES

1. IPCC (Intergovernmental Panel on Climate Change), Climate Change 1995: The Science of Climate Change, J. T. Houghton, L. G. Meira Filho, B. A. Collander, N. Harris, A. Kattenberg, and K. Maskell, eds., Cambridge University Press, Cambridge, UK, 1996.
2. DOE (U.S. Department of Energy), Carbon Sequestration Research and Development, DOE/SC/FE-1, Washington, D.C., 2000.

GLOMALIN: A SOIL PROTEIN IMPORTANT IN CARBON SEQUESTRATION

Sara F. Wright¹, Matthias C. Rillig² and Kristine A. Nichols³

¹USDA-ARS-SMSL, Building 001, Room 140, BARC-W, Beltsville, MD 20705, ²University of Montana, Division of Biological Sciences, HS104, Missoula, MT 59812, ³University of Maryland, Department of Natural Resources and Landscape Architecture, College Park, MD 20742

KEYWORDS: Aggregate stability, soil organic matter, soil stability, glycoprotein

ABSTRACT

Elevated atmospheric CO₂ levels lead to greater fixation of carbon by plants and greater transfer of carbon to roots and soil. We are studying the amplification of a series of events that flow from increased inputs of carbon to plant roots and subsequently to sequestration of organic carbon in soil aggregates. Soil aggregates are groups of primary particles that adhere to each other more strongly than to surrounding soil particles. Plant roots provide carbon for growth and reproduction of a ubiquitous group of symbiotic fungi called arbuscular mycorrhizal fungi (AMF). A recent discovery shows that AMF produce copious amounts of an insoluble, hydrophobic, recalcitrant glycoprotein, named glomalin, which is important in stabilizing soil aggregates. Aggregates store and protect additional organic carbon until the aggregates break down. Thus, greater stability of aggregates leads to larger amounts of protected organic carbon in terrestrial ecosystems.

INTRODUCTION

Increases in atmospheric CO₂ (Keeling et al., 1995) highlight the need to explore ways to trap and sequester this greenhouse gas in terrestrial ecosystems. Plants fix CO₂ and allocate a part of the photosynthate to roots (Rogers et al., 1994) and soil (Jones et al., 1998). Organic carbon in soil plays an important role in soil aggregation (Kemper & Rosenau 1986). Soil aggregates are groups of primary particles that adhere to each other more strongly than to surrounding soil particles (Martin et al., 1955). Relatively labile carbon is protected in soil aggregates (Cambardeila & Elliott 1992; Jastrow & Miller 1997; Six et al., 1998) and has a turnover of 140 – 412 years in a pasture soil, depending upon the aggregate size (Jastrow et al., 1996).

Increased fixation of CO₂ by plants may have a direct effect on root symbionts that utilize plant-fixed carbon for growth – the arbuscular mycorrhizal fungi (AMF). AMF are ubiquitous symbionts of the majority of land plants. AMF are also important in soil aggregate stabilization (Tisdall & Oades, 1982; Jastrow & Miller, 1997). The contribution of AMF to stabilization of aggregates was thought to be through entrapment of soil particles by fungal hyphae, the filamentous structures making up the body of the fungus. Hyphae extend several centimeters from the root into soil. Estimates of AMF extraradical hyphae vary widely (Rillig & Allen, 1999), but one of the highest estimates is 111 m cm³ in a prairie grassland soil (Miller et al., 1995).

A recent discovery of copious production of a glycoprotein, glomalin, by hyphae of AMF (Wright et al., 1996) and its role in aggregate stability (Wright & Upadhyaya 1998) has implications for enhanced carbon sequestration by soils under elevated CO₂. Recently Rillig et al. (1999) provided evidence for a change in aggregate stability under elevated CO₂ in three natural ecosystems. Increases in hyphal length and glomalin concentration in soils were shown concurrently.

This report will review glomalin and aggregate stability: (i) in disturbed and undisturbed agricultural soils, (ii) in agricultural soils in transition from plow- to no-tillage, (iii) in natural grasslands under increased CO₂ and (iv) in a tropical soil. We will also present characteristics of glomalin that indicate the unusual nature of the molecule.

MATERIALS AND METHODS

Glomalin extraction. Extractions were performed as described by Wright & Upadhyaya (1998). One-gram samples of air-dried soil were placed in 8 mL 20 mM citrate, pH 7.0 and autoclaved (121 °C) for 30 min to remove the easily-extractable glomalin (EEG). After centrifugation (10,000 x g) and removal of the supernatant, 8 mL 50 mM citrate, pH 8.0 was added to the remaining soil and heated at 121 °C for 60 min to extract total glomalin (TG). Additional extractions with 50 mM citrate were done until the supernatant was a straw color, indicating that glomalin, a red-brown color, had been removed. One mL of EEG was removed and then the remaining supernatant containing EEG was combined with all of the supernatants from the 50 mM citrate extractions. Protein was determined by the Bradford dye-binding assay with bovine serum albumin as the standard (Wright et al., 1996). An indirect enzyme-linked immunosorbent

assay (ELISA) was used to quantify the immunoreactive fraction (IREEG and IRTG). Weight of soil was corrected for non-aggregated coarse material.

Glomalin purification. Glomalin was precipitated with trichloroacetic acid (TCA) and then dialyzed against 10 mM borate, pH 8.0 as described by Wright et al. (1998). Dialyzed samples were freeze-dried.

Aggregate stability. The apparatus described by Kemper & Rosenau (1996) was used to determine water stability of air-dried aggregates. Air-dried bulk soil was sieved to remove the 1 – 2 mm and 0.5 – 1 mm aggregates. Four g of aggregates was placed in a sieve and pre-wetted by capillary action. The 1 – 2mm aggregates were in 0.25 mm sieves, and the 0.5 – 1 mm aggregates were in a 0.01 mm sieve. Aggregates were pre-wetted by capillary action and then tumbled for 5 min in a column of water. After drying remaining aggregates at 70 °C aggregate stability was calculated: % stability = (g aggregates remaining on the sieve - the coarse material/ 4 g - coarse material) x 100.

Characterization of glomalin. Various routine and specialized assays have been performed to characterize the glomalin molecule. Routine assays are Bradford protein and enzyme-linked immunosorbent assay (ELISA). Methods for these are described above. Sodium dodecyl sulfate polyacrylamide (SDS-PAGE) gel electrophoresis banding patterns on 12% T gels stained with silver are also run on a routine basis (Wright and Upadhyaya, 1996). Iron was analyzed by atomic absorption spectroscopy after microwave digestion in nitric acid.

RESULTS

We have studied undisturbed, disturbed, and soils under elevated CO₂ for the relationship between aggregate stability and glomalin (Rillig et al., 1999; Wright & Upadhyaya, 1998; Wright et al., 1999) in temperate regions. In general, undisturbed soils have the highest aggregate stability and glomalin, but soils appear to differ in the amount of glomalin they can accumulate (Table 1). Both aggregate stability and glomalin are higher in undisturbed compared with disturbed soils (Tables 2 and Fig. 1).

TABLE 1: Selected undisturbed soils that illustrate the range in values for aggregate stability and measures of easily extractable glomalin (EEG), total glomalin (TG), and the immunoreactive fractions of each (IREEG and IRTG, respectively).

Location	Soil Type (series)	Aggregate Stability (%)	TG (mg/g)	IRTG (mg/g)	EEG (mg/g)	IREEG (mg/g)
Maryland	Silt loam (Baltimore)	80	5.2	4.4	2.9	2.5
Virginia	Silt loam (Georgeville)	93	14.1	10.9	10.0	8.3
Illinois	Silty clay loam (Sable)	52	12.6	5.7	4.3	1.9
Minnesota	Sand (Nymore)	55	4.7	8.6	5.8	4.5
Texas [†]	Sandy loam (Berta, Posey)	22	3.3	1.5	1.5	0.6
Colorado [†]	Silt loam (Weld)	60	3.0	1.7	1.0	1.0

[†]Alkaline soils. All other soils are acidic.

Cultivated soils have been compared with undisturbed soil under native or introduced grasses to determine the effects of disturbance on glomalin. The immunoreactive easily extractable (IREEG) fraction of glomalin is most closely correlated with aggregate stability across soil types and locations. This fraction is similar to glomalin on fresh hyphae using currently available analytical procedures (Wright & Upadhyaya, 1998) (Table 2).

TABLE 2: Immunoreactive easily extractable glomalin (IREEG) and aggregate stability of 1 – 2 mm aggregates for three geographic locations with comparisons between disturbed and undisturbed sites (SD in parentheses).

Location	Soil Type	Disturbed		Undisturbed	
		Aggregate stability (%)	IREEG [†] (mg/g)	Aggregate stability (%)	IREEG (mg/g)
Texas [†]	Sandy loam	8.6 (0.6)	0.4 (0.2)	22.3 (3.5)	0.6 (0.2)
Colorado [†]	Silt loam	11.1 (4.3)	1.1 (0.3)	59.9 (20.1)	1.7 (1.4)
Maryland [†]	Silt loam	18.1 (3.0)	0.6 (0.0)	58.9 (3.5)	1.9 (0.3)

[†]Texas – three cultivated sites were compared with three nearby rangeland sites; Colorado – 45 cultivated plots were compared with nine nearby individual grass soils; Maryland – four cultivated plots were compared with four sites from a grass buffer surrounding the plots.

Soil management affects aggregate stability and glomalin. A recent study compared no-tillage to plow-tillage over three years for a silt loam soil in Beltsville, MD corn plots (Wright et al, 1999). Both aggregate stability and glomalin increased during the transition (Fig. 1).

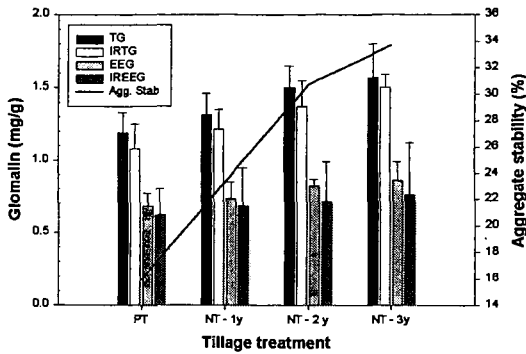


FIGURE 1: Changes in aggregate stability and glomalin during transition from plow- to no-tillage for corn production. TG = total glomalin, EEG= easily extractable glomalin and IR= immunoreactive fraction.

A chronosequence (300 years – 4.1 million years) from Hawaii was studied (manuscript in preparation) to determine glomalin levels in a tropical climate. Very large amounts of TG were found (Fig. 2).

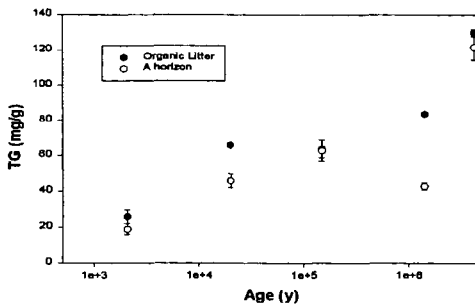


FIGURE 2: Total glomalin in the upper layers of an organic soil chronosequence from Hawaii.

Exposure of annual grassland to elevated CO₂ resulted in increases in the number of aggregates as a proportion of soil mass, and increases in aggregate stability and glomalin (Rillig et al., 1999). Results of this study are summarized in Table 3.

TABLE 3: Effects of increased CO₂ on aggregates as a percent of bulk soil, water stability of aggregates, and glomalin in natural grasslands in California (Rillig et al., 1999).

	Sandstone		Serpentine	
	Ambient CO ₂	Increased CO ₂	Ambient CO ₂	Increased CO ₂
Aggregates 1-2 mm (% of soil)	14.4 (0.5)	15.1 (0.3)	16.7 (0.6)	18.1 (0.5)
Aggregates 0.25-1mm (% of soil)	17.1 (0.6)	20.0 (0.8)	26.9 (1.6)	25.6 (1.1)
Water stable 1-2 mm (%)	86.7 (1.6)	90.1 (1.3)	76.2 (1.5)	81.0 (1.3)
Water stable 0.25-1 mm (%)	88.9 (0.9)	92.8 (0.6)	84.3 (0.9)	85.3 (0.5)
Immunoreactive glomalin (mg/g)	0.7 (0.0)	0.8 (0.0)	1.0 (0.0)	1.1 (0.0)

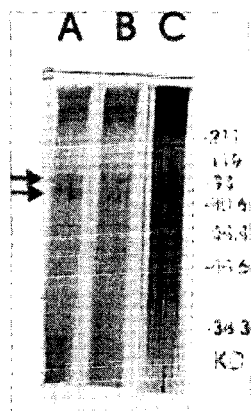
Glomalin is categorized as a glycoprotein (Wright et al., 1998). Carbon, nitrogen, and iron in glomalin from hyphae of two AMF and a soil and other soil are shown in Table 4.

TABLE 4: Total carbon, iron and nitrogen in selected glomalin samples.

Assay	Baltimore soil	Glomus intraradices UT126	Gigaspora rosea FL225
Total Carbon (%)	26.4	24.80	17.50
Fe (%)	7.2	0.5	0.5
N (%)	1.63	1.70	1.22

Similarity between glomalin on hyphae from axenic cultures and soil indicates that the substance extracted from soil is the same as that on hyphae. Raw extracts from hyphae or soil show the same banding patterns on SDS-PAGE (Fig. 3).

FIGURE 3: SDS-PAGE of glomalin extracted from hyphae of *Glomus intraradices* UT126 (A), *Gigaspora gigantea* MA453A (B), and Baltimore soil (C). Molecular weight standards (KD) are indicated. The arrow indicates the position of two bands.



DISCUSSION

Glomalin, a major component of previously unidentified organic matter in soil, reaches levels of 1.4 – 13% of air-dried mineral soils based on Bradford protein values (Table 1, Fig. 2). Comparison of amounts of humic and fulvic acids and glomalin from Hawaiian organic soil on a weight basis show that glomalin can be as high as 26% of the soil while fulvic, humic, and the mineral fraction are 2.7, 6.7, and 60.7%, respectively (unpublished data).

Levels of glomalin in soil are closely associated with aggregate stability. This was shown in undisturbed soils, undisturbed compared with disturbed soils, and during transition from plow- to no-tillage (Tables 1 and 2, Fig. 1). Since glomalin production appears to be directly linked to carbon supplied by plants, production of glomalin may be affected by increased atmospheric CO₂ (Table 3). Evidence for this was also found in a sorghum field equipped with a free-air CO₂ enrichment (FACE) system (manuscript in preparation). Measures of soil AMF hyphal length showed a strong response to CO₂ as well as one fraction of glomalin. Glomalin and AMF hyphal lengths were positively correlated with soil aggregate stability.

The structure of glomalin at present unknown, but the molecule is insoluble, hydrophobic and recalcitrant. Insolubility of the molecule is probably the reason that glomalin was not discovered until recently. We have seen evidence of insolubility and sloughing of glomalin from AMF hyphae in sand cultures of these fungi on plant roots. When cultures are harvested and fresh roots are placed in water, glomalin floats to the surface of the water and collects as a film at the air-water interface. This film entraps air bubbles and adheres to plastic surfaces. Plastic traps have been used to quantify glomalin in cultures (Wright & Upadhyaya, 1999). Residence time of glomalin in soils is currently being investigated, but preliminary results indicate that glomalin in the undisturbed Hawaiian soils (Fig. 2) lasts for 6 – 42 years (manuscript in preparation).

Other fungal proteins, hydrophobins, have characteristics similar to glomalin (Wessels, 1996). For example, the hydrophobin SC3 produced by the basidiomycete *Schizophyllum commune* is a glycoprotein (Wessels, 1997) that is insoluble in hot SDS and forms insoluble complexes (de Vries et al., 1993). Interfacial self-assembly of SC3 monomers leads to insoluble amphiphatic films about 10 nm thick that coat air bubbles (Wessels, 1996). SC3 is secreted from hyphal tips as a monomer and then flows over the hyphal surface as semi-fluid polymers (Wessels, 1996). Hydrophobic interactions of monomers and other bonds may contribute to the overall hydrophobicity of the molecules (Wessels, et al., 1991). Purified SC3 is described as a milky suspension (Wessels, 1997). However, there are no reports of any iron-containing hydrophobins at this time.

Iron in or on glomalin (Table 4) imparts a red-brown color to extracted glomalin, and we think that iron is critical to the stability of the molecule in soil and in laboratory procedures used to reveal the molecular structure. Hydrolysis for amino acid analysis requires 24 h at 150 °C, and a pre-treatment to remove some of the iron may be necessary to achieve complete hydrolysis. We

have successfully removed a large amount of iron from glomalin using 8-hydroxy quinoline, but weaker chelators are slightly effective to ineffective for removal of iron. Lactoferrin is an iron-bearing protein with similarities to glomalin. Lactoferrin is a member of a group of iron-binding glycoprotein called transferrins. Although this glycoprotein is found in animals, it shares some intriguing characteristics with glomalin. Both are approximately the same size (~80 – 90 KD), extracellular, heat and enzymatically stable and difficult to hydrolyze. Lactoferrin hyperaccumulates iron and undergoes conformational changes upon binding iron. We have evidence that glomalin hyperaccumulates iron (Table 4) and are working on dissecting the conformational changes that may occur. Lactoferrin functions in iron binding and transport and as a bacteriostatic molecule – roles that glomalin may play in the soil environment.

Currently we are working to determine amino acid and carbohydrate contents and carbohydrates in glomalin from axenic cultures and soils. This requires stripping the iron with 8-hydroxy quinoline (manuscript in preparation).

CONCLUSIONS

Glomalin is abundant in soils and is closely correlated with aggregate water-stability. Glomalin contains carbon and hence constitutes a non-trivial portion of the terrestrial carbon pool. Possibly far more importantly, however, stabilization of aggregates amplifies the role of glomalin in soils because carbonaceous compounds are protected from degradation inside of aggregates. Increased atmospheric CO₂ can lead to increased production of glomalin because of the symbiotic association that exists between plants and producers of glomalin, AMF. We have also shown that glomalin concentrations in soils are influenced by management practices, for example in agroecosystems, further highlighting the role of this protein in carbon storage. Glomalin is an unusual molecule that has proven difficult to analyze biochemically due to its recalcitrance and possible complexity. Future research will be directed towards the elucidation of its structure and the controls on its production.

REFERENCES

- Cambardella, C. A., & Elliott, E. T. (1992) *Soil Sci. Soc. Am. J.* 56, 777-783.
- De Vries, O. M. H., Fekkes, M. P., Wösten, H. A. B., & Wessels, J. G. H. (1993) *Arch. Microbiol.* 159, 330-335.
- Jastrow, J. D., & Miller, R. M. (1997) *Soil Processes and the Carbon Cycle*, pp 207-223, CRC Press, Boca Raton, FL.
- Jastrow, J. D., Boutton, T. W., & Miller, R. M. (1996) *Soil Sci. Soc. Am. J.* 60, 801-807.
- Jones, T. H., Thompson, L. J., Lawton, H. H., Bezemer, T. M., Bardgett, R. D., Blackburn, T. M., Bruce, K. D., Cannon, P. F., Hall, G. S., Hartley, S. E., Howson, G., Jones, C. G., Kampichler, C., Kandeler, E., & Ritchie, D. A. (1998) *Science* 280, 441-443.
- Keeling, C. D., Whorf, T. P., Whalen, M., & van der Plicht, J. (1995) *Nature* 375, 666-670.
- Kemper, W. D., & Rosenau, R. C. (1986) *Methods of Soil Analysis (Part I)*, pp. 425-442, American Society of Agronomy, Madison, WI.
- Martin, J. P., Martin, W. P., Page, J. B., Ranley, W. A., & De Ment, J. D. (1955) *Adv. Agro.* 7, 1-37.
- Miller, R. M., Reinhardt, D. R., & Jastrow, D. D. (1995) *Oecologia* 103, 17-23.
- Rillig, M. C., & Allen, M. F. (1999) *Mycorrhiza* 9, 1-8.
- Rillig, M. C., Wright, S. F., Allen, M. F., & Field, C. B. (1999) *Nature* 400, 628.
- Rogers, H. H., Runion, G. B., & Krupa, S. V. (1994) *Environ. Pollution* 83, 155-189.
- Wessels, J. G. H. (1996) *Trends Plant Sci.* 1, 9-15.
- Wessels, J. G. H. (1997) *Adv. Microbial Physiol.* 38, 1-45.
- Wessels, J. G. H. de Vries, O. M. H., Åsgeirsdóttir, & Schuren, F. H. J. (1991) *Plant Cell* 3, 793-799.
- Six, J., Elliott, E. T., Paustian, K., & Doran, J. W. (1998) *Soil Sci. Soc. Am. J.* 62, 1367-1377.
- Tisdall, J. M., & Oades, J. M. (1982) *J. Soil Sci.* 33, 141-163.
- Wright, S. F., & Upadhyaya, A. (1996) *Soil Sci.* 161, 575-586.
- Wright, S. F., & Upadhyaya, A. (1998) *Plant Soil* 198, 97-107.
- Wright, S. F., & Upadhyaya, A. (1999) *Mycorrhiza* 8, 283-285.
- Wright, S. F., Upadhyaya, A., & Buyer, J. S. (1998) *Soil Biol. Biochem.* 30, 1853-1857.
- Wright, S. F., Starr, J. S., & Paltineanu, I. C. (1999) *Soil Sci. Soc. Am. J.* 63, 1825-1829

PROCESS MODELING OF CO₂ INJECTION INTO NATURAL GAS RESERVOIRS FOR CARBON SEQUESTRATION AND ENHANCED GAS RECOVERY

C.M. Oldenburg, K. Pruess, and S.M. Benson
Earth Sciences Division
Lawrence Berkeley National Laboratory
Berkeley, CA 94720

KEYWORDS: carbon sequestration, enhanced gas recovery, natural gas reservoir

ABSTRACT

Injection of CO₂ into depleted natural gas reservoirs offers the potential to sequester carbon while simultaneously enhancing CH₄ recovery. Enhanced CH₄ recovery can partially offset the costs of CO₂ injection. With the goal of analyzing the feasibility of carbon sequestration with enhanced gas recovery (CSEGR), we are investigating the physical processes associated with injecting CO₂ into natural gas reservoirs. The properties of natural gas reservoirs and CO₂ and CH₄ appear to favor CSEGR. In order to simulate the processes of CSEGR in detail, a module for the TOUGH2 reservoir simulator that includes water, brine, CO₂, tracer, and CH₄ in nonisothermal conditions has been developed. Simulations based on the Rio Vista Gas Field in the Central Valley of California are used to test the feasibility of CSEGR using CO₂ separated from flue gas generated by the 680 MW Antioch gas-fired power plant. Model results show that CO₂ injection allows additional methane to be produced during or after CO₂ injection.

INTRODUCTION

Depleted natural gas reservoirs are potentially important targets for carbon sequestration by direct carbon dioxide (CO₂) injection. The accumulation and entrapment of a light gas such as methane (CH₄) testifies to the integrity of natural gas reservoirs for containing gas for long periods of time. By virtue of their proven record of gas production, depleted natural gas reservoirs have demonstrated histories of both (i) available volume, and (ii) integrity against gas escape. The IEA (International Energy Agency) has estimated that as much as 140 GtC could be sequestered in depleted natural gas reservoirs worldwide (IEA, 1997) and 10 to 25 GtC in the U.S. alone (Riechle et al., 2000). These aspects of natural gas reservoirs for carbon sequestration are widely recognized.

Less well recognized is the potential utility of CO₂ injection into natural gas reservoirs for the purpose of enhancing CH₄ production by simple repressurization of the reservoir. The pressure support provided by the CO₂ is similar to the proven cushion gas concept used in the gas storage industry wherein expansion of cushion gases upon natural gas withdrawal aids in production from the storage reservoir (Carrière et al., 1985; Laïlle et al., 1988). The concept of enhancing CH₄ production is important because it can partially offset the costs of CO₂ sequestration. This concept was first described by van der Burgt et al. (1992) and Blok et al. (1997), who used reservoir simulation to evaluate how quickly the injected CO₂ would mix with the produced natural gas. Based on the simulations they concluded that enhanced production was possible for some period before the extent of mixing was too great. Nevertheless, little attention has been given to this option for sequestration, primarily due to concerns about degrading the quality of the produced gas.

The purpose of this paper is to further explore the physical processes involved in CSEGR. To accomplish this, numerical simulations of CO₂ injection and enhanced gas recovery were carried out on a model system based on the Rio Vista Gas Field in California's Central Valley. The proposed source of CO₂ in this study is flue gas from the 680 MW power plant at Antioch, California, 20 km from Rio Vista. To carry out the simulations, we have developed capabilities for the TOUGH2 reservoir simulator (Pruess et al., 1999) for modeling gas reservoirs. Through simulations of the injection process, we show that repressurization of the methane is possible and significant quantities of methane that would otherwise be left in the reservoir can be produced while carbon dioxide is being injected.

PROCESS DESCRIPTION

CSEGR involves the injection of CO₂ into depleted gas reservoirs with simultaneous or subsequent production of repressurized CH₄. The processes of gas-phase mixing by advection, dispersion, and molecular diffusion, which will tend to mix the gaseous components and deteriorate the quality of the natural gas, are dependent on the properties of natural gas reservoirs and of the gases. Pressures in depleted natural gas reservoirs are approximately 20–50 bars, with temperatures 27–120 °C. The large volume and large areal extent of gas reservoirs decrease the potential for mixing by dispersion over practical time scales. In Table 1 we present properties of CO₂ and CH₄ relevant to CSEGR. Note that CO₂ is denser and more viscous than CH₄, and will generally be subcritical but may be supercritical in deep depleted reservoirs. The large density of CO₂ relative to CH₄ means that CO₂ will tend to migrate downwards relative to CH₄. The larger viscosity of CO₂ ensures that displacement of CH₄ by CO₂ will be a favorable mobility ratio displacement, with less tendency for the gases to finger and intermix than in displacements such as water floods in oil reservoirs. Pressure diffusivity is typically three–five orders of magnitude larger than molecular diffusivity, making repressurization occur much faster than mixing by molecular diffusion. In summary, the properties of gas reservoirs and CO₂ and CH₄ appear to favor the feasibility of CSEGR.

Table 1. Properties of CO₂ and CH₄ from Vargaftik (1975).

Property	CO ₂	CH ₄
Molecular weight	44 g/mole	16 g/mole
Critical point	31 °C, 73 bar	-83 °C, 46 bar
Density	880 kg/m ³ (50 °C, 300 bar) 140 kg/m ³ (50 °C, 60 bar)	193 kg/m ³ (50 °C, 300 bar) 39 kg/m ³ (50 °C, 60 bar)
Viscosity	0.085 cp (50 °C, 300 bar) 0.019 cp (50 °C, 60 bar)	0.023 cp (50 °C, 300 bar) 0.013 cp (50 °C, 60 bar)
Diffusivity (at 273 K, 1 bar)	1.42 x 10 ⁻⁵ m ² /s (in air)	1.53 x 10 ⁻⁵ m ² /s (in CO ₂)

MATHEMATICAL MODEL

In order to model gas reservoir processes, we have developed a module called EOS7C (Oldenburg and Pruess, 2000) for simulating gas and water flow in natural gas reservoirs within the TOUGH2 framework (Pruess et al., 1999). The module handles five components (water, brine, non-condensable gas, tracer, and methane) along with heat. The non-condensable gas can be selected by the user to be CO₂, N₂, or air. EOS7C is an extension of the EOS7R (Oldenburg and Pruess, 1995) and EWASG (Battistelli et al., 1997) modules. The EOS7C module is currently restricted to the high-temperature "gas-like" conditions for CO₂, as opposed to the high-pressure "liquid-like" conditions. Advection of gas and liquid phases is governed by a multiphase extension of Darcy's law. Molecular diffusion in the gas and liquid phases is currently modeled using a Fickian approach. The main gas species partition between the gas and liquid phases according to their temperature- and pressure-dependent solubilities (Irvine and Liley, 1984; Cramer, 1982; Pritchett, 1981), while the gas tracer volatilization is controlled by a Henry's coefficient input by the user. The selection of N₂ or air in place of CO₂ will allow the module to be used for simulating gas storage processes, including the use of inert cushion gases. Because it is a module of TOUGH2, EOS7C includes all of the multiphase flow capabilities of TOUGH2, including the ability to model water drives and gas-liquid displacements that may be present in gas reservoirs.

APPLICATION TO RIO VISTA GAS FIELD

In this section, we investigate by numerical simulation the process of CSEGR at the Rio Vista Gas Field. Rio Vista is the largest gas field in California and has been under production since 1936 (Burroughs, 1967). It is located approximately 75 km north of San Francisco in the Sacramento Basin and has an elongated dome-shaped structure extending over a 12 by 15 km area (see Figure 1). The reservoir rocks are Upper Cretaceous to Eocene and consist of alternating layers of sands and shales deposited in deltaic and marine environments. Normal faulting occurred contemporaneously with sedimentation, creating a set of sub-parallel faults trending NW through the field. The most important of these is the Midland Fault (Figures 1 and 2). In some gas-bearing strata, displacement along the faults has created structural traps. In others, particularly the thicker gas bearing sands, the smaller faults do not play as important a role in defining reservoir structure.

Since 1936 the Rio Vista Gas Field has produced over 9.3×10^{10} m³ of natural gas (at standard conditions of 1 bar, 15.5 °C [14.7 psi, 60 °F]) from 365 wells. Production peaked in 1951 with annual production of 4.4×10^9 m³ and, as shown in Figure 3, has declined steadily since then (Cummings, 1999). Production decline is caused by decreasing reservoir pressures and increased water production, particularly on the western boundary of the field.

The Domengine formation shown in Figure 2 has been the most productive pool in the Rio Vista Gas Field. It occurs at an average depth of 1150 to 1310 m with an average net thickness of 15 to 100 m. The initial reservoir pressure and temperature were approximately 120 bars and 65 °C. Other generalized reservoir properties are provided in Table 2. As shown in Figure 2, the Domengine is laterally continuous across the Rio Vista Gas Field with vertical confinement provided by the Nortonville and Capay Shales. Its western boundary is controlled by the presence of the watertable at a depth of 1325 m. For the purpose of this study we focused on CO₂ sequestration and enhanced gas recovery in the Domengine formation to the west of the Midland Fault (see Figure 4).

The source of CO₂ considered in this study is the 680 MW gas-fired power plant located in Antioch, California (20 km from Rio Vista). This plant produces 2.2×10^9 m³ (1 bar, 15.5 °C) or 4.15×10^9 kg of CO₂ annually. At this rate, a simple volumetric replacement of all of the natural gas produced from Rio Vista since 1936 suggests that approximately 80 years of sequestration capacity are available.

The simplified 2-D model system based on the Rio Vista Gas Field is shown in Figure 4. The model system is a 1 km wide cross-section with vertical dimensions 100 m and horizontal extent 6600 m of the western flank of the dome, corresponding to 1/16 of the actual length of the reservoir. The model reservoir has a roof sloping at 0.78 ° and closed right-hand side. The bottom of the gas reservoir is a horizontal water table. Note that in all simulations presented here, water drive is turned off by closing all the lower boundaries of the system. Properties of the formation are simplified for this study as shown in Table 3.

Table 2. Relevant properties of Rio Vista model gas reservoir.

Property	Value	Units
Porosity	0.35	-
Y-, Z-direction permeability	1.0×10^{-12} , 1.0×10^{-14}	m^2 , m^2
Capillary pressure $m, S_{lr}, 1/\alpha, P_{capmax}, S_{li}$	van Genuchten (1980); 0.2, 0.27, 8.4×10^{-4} , $\cdot 10^5$, 1.	-, -, Pa^{-1} , Pa, -
Relative permeability liquid gas	Van Genuchten model Corey model ($S_{gr} = 0.01$)	- -
Molecular diffusivity in gas, liquid	1.0×10^{-3} , 1.0×10^{-10}	$\text{m}^2 \text{s}^{-1}$, $\text{m}^2 \text{s}^{-1}$
Temperature	65	$^{\circ}\text{C}$
Initial pressure at water table	126	bars

The initial condition consists of the water table at $Z = 0$ on the left-hand side of the domain at a pressure of 126 bars, with CH_4 gas and residual water ($S_w = 0.27$) in the pore space above. All simulations were done at isothermal conditions of 65°C . From this initial condition, we simulated the withdrawal of CH_4 at 1/16 the historical rate as shown in Figure 3 for the period 1936–1998.

Following the historical production, we simulated CO_2 injection at a point 15 m below the top of the reservoir at approximately $Y = 2000$ m, and CH_4 withdrawal from the upper right-hand side of the domain ($Y = 6600$ m). In all cases, CO_2 is injected into the reservoir at a rate corresponding to 1/16 the actual production of CO_2 from the 680 MW Antioch gas-fired power plant. An example simulation result is shown in Figure 7 where we show mass fraction of CO_2 along with gas velocity vectors at three different times for the case of CO_2 injection with no CH_4 production. Note the depression of the water table in response to gas injection. As gas is injected, reservoir pressure increases with limited mixing of the gases by advection and diffusion.

Summaries of the simulated pressure evolutions and mass production rates are shown in Figures 5 and 6, respectively. We simulated two different scenarios that start in 1999 (see Table 3). In Scenario I, CO_2 is injected into the reservoir for ten years starting in 1999, as shown in Figure 7. This injection serves to repressurize the reservoir. In the subsequent part of Scenario I, CH_4 is produced for ten years from the repressurized reservoir at a rate corresponding to the 1950–1960 average rate. In Scenario II, CO_2 injection is simultaneous with CH_4 production, where CH_4 is produced at constant pressure. Note in Figure 5 that in Scenario I, 99% pure CH_4 can be produced for about 5 years following CO_2 injection, and that this CH_4 production is at a very large rate. In Scenario II, 99% pure CH_4 can be produced for approximately 10 years during CO_2 injection, although the rate is smaller than in Scenario I (see Figure 6). Note that these simulations have neglected dispersion which would increase gas-phase mixing. Assuming a longitudinal dispersivity of 100 m and 20 years of CSEGR, the dispersive mixing length for these scenarios is on the order of 1 km. This estimate shows that dispersion is an important mixing mechanism, but that over the large length scale in the model gas reservoir, repressurization and production of high quality methane would still be possible. The total additional masses of CH_4 produced by CSEGR for Scenarios I and II are 1×10^9 kg (5.2×10^7 Mcf) and 1.1×10^9 kg (5.7×10^7 Mcf), respectively, as compared to a projected 1.8×10^8 kg (9.4×10^6 Mcf) without CSEGR. Note that these quantities are for the 2-D model system which is 1/16 of the whole gas field.

Table 3. CSEGR scenarios for Rio Vista case study.

Period	Inject	Produce	Rate	Cumulative mass
1936–1998	-	CH_4	Variable (1/16 historical CH_4 production)	-3.5×10^9 kg CH_4
Scenario I. 1999–2009	CO_2	-	8.2 kg/s (1/16 Antioch CO_2 production)	2.6×10^9 kg CO_2
2010–2019	-	CH_4	3.2 kg/s (1950–1960 average rate)	-9.6×10^8 kg CH_4
Scenario II. 1999–2019	CO_2	CH_4	CO_2 : 8.2 kg/s CH_4 : Variable (constant pressure of 39 bars)	5.1×10^9 kg CO_2 -1.1×10^9 kg CH_4

Finally, we present in Figure 8 a scenario to examine the process of density stratification within the reservoir for the case of no CH_4 production. In this scenario, CO_2 is injected for 10 years and then allowed to migrate as driven by density and pressure gradients. As seen in Figure 8, CO_2 moves downwards due to its greater density relative to CH_4 , a process favorable for CSEGR.

CONCLUSIONS

The Rio Vista Gas Field is a potential site for CSEGR. Properties of natural gas reservoirs and of CO_2 and CH_4 are favorable for repressurization without extensive mixing over time scales of practical interest. Simulations of the process of CO_2 injection into a depleted natural gas reservoir carried out with TOUGH2/EOS7C confirm the plausibility of CSEGR as a way to sequester carbon while enhancing methane recovery. Simulations that use realistic estimates of CO_2 produced from the Antioch gas-fired power plant show that with CSEGR, more than five times the mass of methane can be recovered relative to that which would be produced without CSEGR.

ACKNOWLEDGMENTS

The authors would like to thank Drs. P. Witherspoon and L. Myer of Lawrence Berkeley National Laboratory for fruitful discussions regarding the feasibility of carbon sequestration and enhanced gas recovery. We would also like to acknowledge the help of M. F. Cummings of the California Division of Oil and Gas in obtaining detailed production data for the Rio Vista Gas Field. Thanks are also due to Victoria Porto who helped gather the early data needed for this project. This work was supported by Laboratory Directed Research and Development Funds at Lawrence Berkeley National Laboratory under Department of Energy Contract No. DE-AC03-76SF00098.

REFERENCES

- Battistelli, A., C. Calore, and K. Pruess, The simulator TOUGH2/EWASG for modelling geothermal reservoirs with brines and non-condensable gases, *Geothermics*, 26(4), 437-464, 1997.
- Blok, K., R.H. Williams, R.E. Katofsky, and C.A. Hendriks, Hydrogen production from natural gas, sequestration of recovered CO₂ in depleted gas wells and enhanced natural gas recovery, *Energy*, 22 (2,3), 161-168, 1997.
- Bondor, P.L., Applications of carbon dioxide in enhanced oil recovery, *Energy Convers. Mgmt.*, 33 (5-8), 579-586, 1992.
- Bouroughs, E., Rio Vista Gas Field. Summary of California oil fields, Vol. 53., No. 2-Part 2., pp. 25-33, State of California, Department of Conservation, Division of Oil and Gas, 1967.
- Carrière, J.F., G. Fasanino, and M.R. Tek, Mixing in underground storage reservoirs, *Society of Petroleum Engineers SPE-14202*, 9-12, 1985.
- Cramer, S.D., The solubility of methane, carbon dioxide and oxygen in brines from 0° to 300°C, U.S. Bureau of Mines, Report No. 8706, 16 pp., 1982.
- Cummings, M. F., Northern California oil and gas field production. Annual production and well Data. 1977-1998. State of California, Division of Oil, Gas and Geothermal Resources, 1999.
- IEA, Carbon Dioxide Utilization, IEA Greenhouse Gas R&D Programme, Table 6, 1997.
- Irvine, T.F. Jr., P.E. Liley, Steam and gas tables with computer equations, Academic Press, Orlando, FL, 185 pp, 1984.
- Laille, J-P., J-E. Molinard, and A. Wents, Inert gas injection as part of the cushion of the underground storage of Saint-Clair-Sur-Epte, France, *Society of Petroleum Engineers SPE-17740*, 343-352, 1988.
- Mualem, Y., A new model for predicting the hydraulic conductivity of unsaturated porous media, *Water Resour. Res.*, 12(3), 513-522, 1976.
- Oldenburg, C.M., and K. Pruess, EOS7R: Radionuclide transport for TOUGH2, Lawrence Berkeley National Laboratory Report, LBL-34868, 1995.
- Oldenburg, C.M., and K. Pruess, EOS7C: Gas reservoir simulation for TOUGH2, Lawrence Berkeley National Laboratory Report, in preparation, 2000.
- Pruess, K., C. Oldenburg, and G. Moridis, TOUGH2 user's guide, version 2.0, Ernest Orlando Lawrence Berkeley National Laboratory Report, LBNL-43134, November 1999.
- Pritchett, J.W., M.H. Rice, and T.D. Riney, Equation-of-state for water-carbon-dioxide mixtures: implications for Baca reservoir, Report DOE/ET/27163-8, UC-66-a, 53 pp, 1981.
- Riechle et al., Carbon sequestration research and development. U.S. Department of Energy, DOE/SC/FE-1, 2000.
- van der Burgt, M.J., J. Cantele, and V.K. Boutkan, Carbon dioxide disposal from coal-based IGCCs in depleted gas fields, *Energy Convers. Mgmt.*, 33 (5-8), 603-610, 1992.
- van Genuchten, M.Th., A closed form equation for predicting the hydraulic conductivity of unsaturated soils, *Soil Sci. Soc.*, 44, 892-898, 1980.
- Vargaftik, N.B., Tables on the thermophysical properties of liquids and gases, 2nd Ed., John Wiley & Sons, New York, NY, 1975.

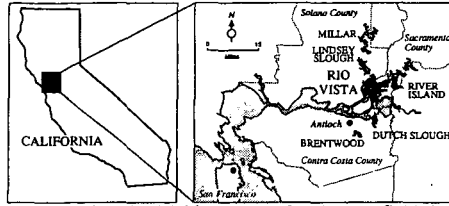


Figure 1. Rio Vista Gas Field area map showing gas fields in black.

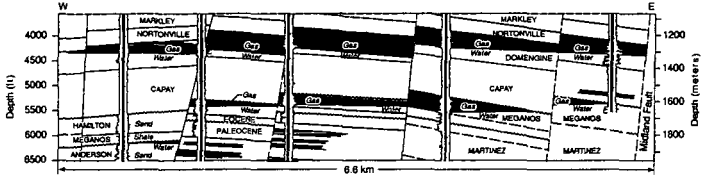


Figure 2. East-west cross section of the Rio Vista Gas Field modified from Burroughs (1967).

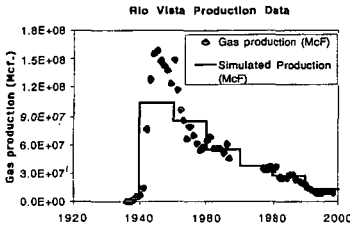


Figure 3. Production history of methane from the Rio Vista Gas Field. Production from model system is 1/16 of the 10-year-averages shown. (n.b., 1 Mcf = 10^3 cf)

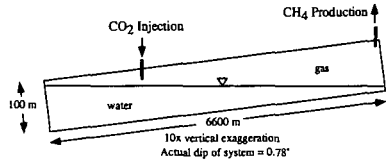


Figure 4. 2-D vertical section used in CSEGR simulations.

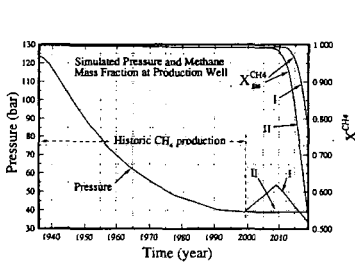


Figure 5. Pressure and CH_4 mass fraction evolution for Scenarios I and II.

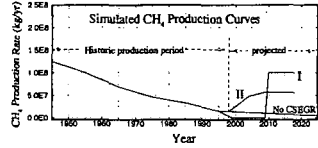


Figure 6. Simulated mass production rates of CH_4 for Scenarios I, II, and projected if no CSEGR.

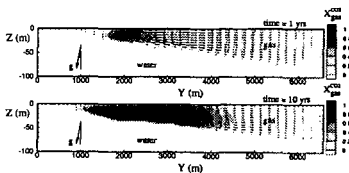


Figure 7. Mass fraction of CO_2 in the gas phase and gas velocity at $t = 1$ yr and 10 yrs with no CH_4 production.

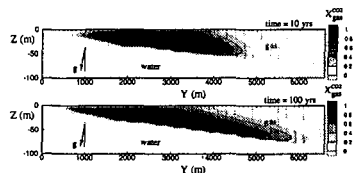


Figure 8. Mass fraction CO_2 in the gas phase and gas velocity at $t = 10$ yrs and 100 yrs for the case of gravity-driven density stratification following 10 years of CO_2 injection.

FIELD-TESTING CO₂ SEQUESTRATION AND ENHANCED COALBED METHANE RECOVERY IN ALBERTA, CANADA – A HISTORICAL PERSPECTIVE AND FUTURE PLANS

William D. Gunter and Sam Wong, Alberta Research Council, 250 Karl Clark Road, Edmonton, AB, Canada T6N 1E4; and Thomas Gentzis, National Centre for Upgrading Technology, 1 Oil Patch Drive, Suite A202, Devon, AB, Canada T9G 1A8

ABSTRACT

The Alberta Research Council is leading a program on the reduction of greenhouse gas emissions by injecting CO₂, N₂, and flue gas in a deep coal seam while enhancing the recovery factors and production rates of methane. A field test was carried out in 1998 to obtain accurate information on CO₂ storage and production of CH₄ following a CO₂ injection/soak period. Experimental data was used to calibrate simulation models for a feasibility analysis of a full-scale, 5-spot pilot study planned for 2000-2002. In late 1999, a new well was drilled and completed in order to perform a simulated flue gas micro-pilot test into the coal seam. Three additional well may be drilled in 2001. Subsequently, gases will be injected into the four wells and production will be monitored from a fifth well over a 12-month period. Full-scale commercial development could begin as early as 2003.

KEYWORDS: Coalbed methane recovery, CO₂ storage, Alberta Basin

INTRODUCTION

The coalbed methane (CBM) recoverable resources in the Plains and Foothills regions of the Western Canada Sedimentary Basin (WCSB) are estimated to be 135 to 261 trillion cubic feet (TCF) and are comparable to the marketable conventional gas endowment of 263 TCF (1). About 48.5 megatonnes (Mt) or 32% of the 151 Mt of CO₂ emissions generated in Alberta in 1996 originated from coal-fired power plants (Figure 1). The above figure also shows that coal beds in the Alberta part of the WCSB are second only to aquifers in terms of storage capacity for CO₂ (2). An abundance of deep and unminable coal seams in Alberta makes geological storage of CO₂ applicable, particularly in those areas located in close proximity to power plants emitting large quantities of CO₂, a greenhouse gas (GHG). In such a storage process, the CO₂ produced from the power plants could be injected into the coal seams to produce CBM. This could lead to null-GHG power plants that would be fuelled by methane released from the deep coals in a cyclical approach that would eliminate any release of CO₂ to the atmosphere.

The Alberta Research Council is currently leading a multi-phase study on field-testing CO₂-enhanced CBM recovery at a site near Fenn Big Valley, Alberta, Canada. Phase I encompassed a paper study of the initial assessment and proof of concept of injecting CO₂, nitrogen, and flue gas into Mannville Group coals (Lower Cretaceous age) in the Alberta Basin. Phase II concentrated on the design and implementation of a CO₂-micro-pilot test following procedures developed by Amoco Production Company for coals in the San Juan Basin in the U.S. The project is now in Phase III, which is to evaluate the design and implementation of a full-scale pilot project. Burlington Resources has successfully injected CO₂ into relatively high permeability coal seams in the San Juan Basin and stimulated CBM production and recovery rates compared to primary production (a pressure depletion process). Additional tests are needed to demonstrate the concept for the low permeability coals of the Alberta Basin and elsewhere in the world.

RESULTS AND DISCUSSION

Following the successful completion of Phase I in the summer of 1997, Phase II proceeded in a timely manner and was completed in the spring of 1999. The primary goals of Phase II were the following: (1) to accurately measure data from a single well test involving a series of CO₂ injection/soak cycles followed by production of CO₂ and methane; (2) to history match the measured data with a comprehensive coal gas reservoir simulation model in order to obtain estimates of reservoir properties and sorption characteristics; and (3) to calibrate simulation models to predict the behaviour of a large-scale pilot project or full field development. The field test was carried out in an existing Gulf Canada well at the Fenn Big Valley location in the central Alberta Plains. Phase II was, in essence, the prelude to a full-scale 5-spot pilot test. The study concluded that a

full-scale pilot CO₂ sequestration/ECBM (enhanced coalbed methane recovery) project is possible in the above location (3).

The economic feasibility analysis of Phase II revealed that flue gas injection offers better economic return than pure CO₂ injection unless there is credit for the CO₂ avoided. At a rate of US\$1.00 per thousand standard cubic feet (MSCF) of CO₂ (US\$19 per tonne), the CO₂ would account for US\$2.00 per MSCF of methane sold, assuming that it takes at least 2 cubic feet of CO₂ injected for each cubic feet of methane produced. The CO₂-ECBM recovery mechanism is shown in Figure 2 (4-5). It might be advantageous to optimize the CO₂/N₂ composition of the flue gas when considering CO₂ storage/sequestration options. If flue gas is injected, the CO₂ would remain sorbed in the coal matrix while the majority of N₂, by being adsorbed less than CO₂, would be produced along with the methane. Flue gas injection would enhance CBM production rates by more than a factor of two (6). However, the early breakthrough of N₂ at the production well will cause an additional expense of having to separate N₂ from methane for sales. Pressure swing adsorption (PSA) systems are the optimum method to remove N₂ from the produced gas for small-scale/large N₂ content operations whereas cryogenic processes are favored for large field operations (7). Flue gas conditioning, compression, and N₂/CH₄ separation in surface facilities remain some of the technical challenges that will be addressed in Phase III.

Therefore, by combining CO₂ and N₂ for injection, the appearance of N₂ will be retarded compared to a pure N₂ injection stream and the methane production rate will be enhanced compared to a pure CO₂ stream [6]. However, gas separation will play a key role in the production of methane from coal beds and the most economic gas separation method for the injection gas stream will depend on the specified CO₂ concentration of this stream (7).

The three numerical models that were evaluated in Phase II adequately predicted the primary production of CBM. One such simulation, based on a 5-spot, 320-acre pattern, showed that CH₄ production rate increased by a factor of about 5 compared to primary production when flue gas was injected but methane production decreased rapidly (Figure 3). On the other hand, pure CO₂ injection resulted in methane production at lower rates but for much longer periods of time. Only one out of the three models evaluated was suitable to simulate flue gas injection. None of the three simulation software packages were capable of predicting the produced gas composition in the field test with any degree of accuracy. A better understanding of the process mechanisms involved, for example multiple gas sorption and diffusion, and changes in coal matrix volume due to sorption/desorption of gases is needed to guide any future development of the models.

Phase III was divided in two parts, to be conducted in stages from 1999 to 2001. Phase III-A evaluated the options for the treatment of flue gas, compression and associated economics to optimize CO₂ storage and CBM recovery both at the pilot and commercial scales. A second well was drilled and completed in the fall of 1999. Two flue gas micro-pilot tests, first of this kind in the world that involve injection of flue gas into a coal seam were carried out. Initially, core samples were taken from the second well and evaluated to determine the gas-in-place volume, gas composition, and gas storage capacity. The micro-pilot test was performed in the spring of 2000 by injecting a simulated flue gas steam consisting of two different ratios of N₂ and CO₂ to obtain greater methane recovery without any hindrance to CO₂ storage. The data will be used to finalize the design of the full-scale project that will be implemented in Phase III-B.

Phase III-B encompasses the implementation of a 5-spot field pilot, which would consist of four injection wells and one production wells, sized in a rectangular pattern between 20 and 40 acres. The objective of this phase would be to demonstrate the viability of a large-scale CO₂ storage/ECBM project and to obtain information on the specifications of the technology required to perform a full-scale development project. These specifications will be used to design flue gas collection and treatment facilities, compression, and gas production/separation facilities. The current plans call for the 5-spot pilot to be performed in the Fenn Big Valley site. Three additional wells will be drilled in 2001. These wells, along the one drilled in 1999 and the existing Gulf Canada well will comprise the 5 wells needed for the large pilot. Injection will begin in 2001 and will continue for 12 months.

If the large-scale pilot is successful, full-scale development could begin in 2003 either on the above site or at another suitable location in the Alberta Basin.

Although most of the work so far has focused on the Manville Group coals in the Fenn Big Valley area, a parallel study conducted by the Geological Survey of Canada evaluates the geological properties of other unminable coal seams in Alberta, such as those of the Edmonton and the Ardley groups (Upper Cretaceous-Lower Tertiary). The Edmonton coals are shallower than the Mannville coals and are located in closer proximity to major coal-fired power plants, thus making these coals favourable targets for CO₂ storage. On the other hand, the Ardley coals are being investigated because of their higher permeability and lower injection pressures and costs required for a successful pilot.

CONCLUSION

In conclusion, flue gas injection into coalbed reservoirs has scientific merit and is more economical than pure CO₂ injection for ECBM recovery purposes. Existing information on any field experience of injecting flue gas into geological formations is scarce. More work is needed on the gas treating, compression, and injection methods in order to allow us to determine the economics between CO₂ storage and methane production from coal beds.

REFERENCES

1. Natural Gas Potential in Canada, a Report by the Canadian Gas Potential Committee, 1997.
2. Gunter, W.D., Wong, S., Cheel, D.B., and Sjostrom, G. Large CO₂ sinks: their role in the mitigation of greenhouse gases from an international, national (Canadian) and provincial perspective, *Applied Energy*, **61**, 209 (1998).
3. Wong, S., and Gunter, W.D. Testing CO₂-enhanced coalbed methane recovery, International Energy Agency Gas R & D Program, Greenhouse Issues, (45), November 1999, p. 1-3.
4. Wong, S., Foy, C., Gunter, W.D., and Jack, T. Injection of CO₂ for enhanced energy recovery: Coalbed methane versus oil recovery, Proc. 4th Int. Conf. on GHG Control Technologies, Interlaken, Switzerland (Reimer, P., Eliason B., and Wokaum, A. Eds.), 189, Pergamon, 1999.
5. Wong, S., Gunter, W.D., and Mavor, M.J. Economics of CO₂ sequestration in coalbed methane reservoirs, Proc. SPE/CERI Gas Technol. Symp. 2000, SPE 59785, April 3-5 2000, Calgary, Alberta, 631.
6. Wong, S., Gunter, W.D., Law, D., and Mavor, M.J. Economics of flue gas injection and CO₂ sequestration in coalbed methane reservoirs, Proc. 5th Int. Conf. on GHG Control Technologies, Cairns, Australia, August 13-16, 2000.
7. Ivory, J., Gunter, W.D., Law, D., Wong, S., and Feng, X., Recovery of CO₂ from flue gas, CO₂ sequestration, and methane production from coalbed methane reservoirs, Proc. Int. Symp. on Economaterials, Ottawa, Canada, August 20-23, 2000.

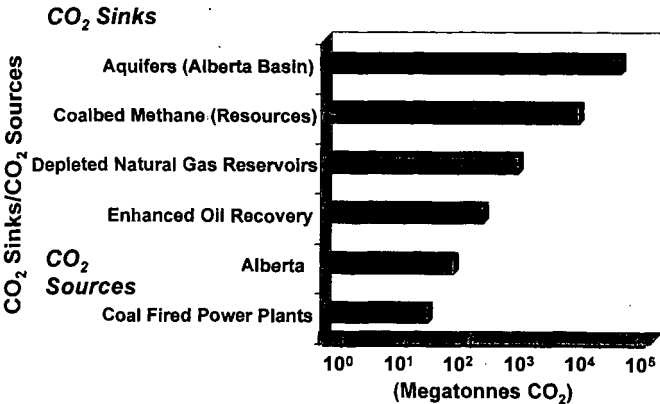


Figure 1 Emissions and greenhouse gas storage capacity in the Alberta basin.

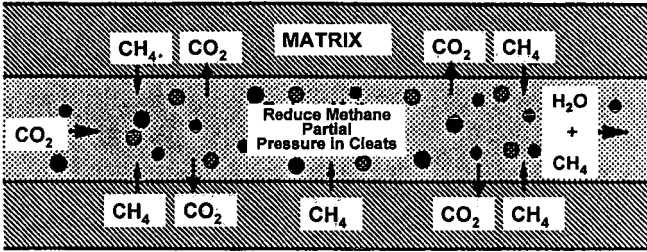


Figure 2 CO₂-enhanced coalbed methane recovery mechanism.

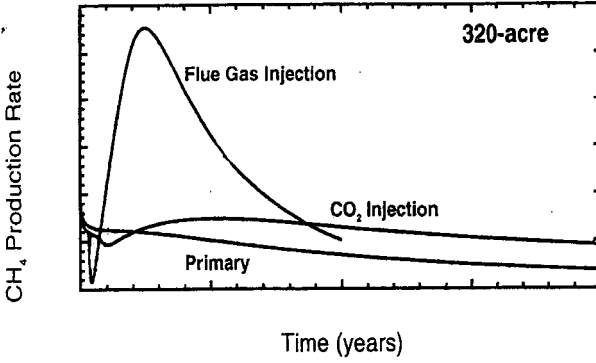


Figure 3 Coalbed methane production rate over time for primary recovery and as a result of pure CO₂ and flue gas injection.